

Review

Forest and Crop Leaf Area Index Estimation Using Remote Sensing: Research Trends and Future Directions

Jin Xu ¹, Lindi J. Quackenbush ^{1,*}, Timothy A. Volk ²  and Jungho Im ³ ¹ Department of Environmental Resources Engineering, State University of New York College of Environmental Science and Forestry, Syracuse, NY 13210, USA; jxu145@syr.edu² Department of Sustainable Resources Management, State University of New York College of Environmental Science and Forestry, Syracuse, NY 13210, USA; tavolk@esf.edu³ School of Urban and Environmental Engineering, Ulsan National Institute of Science and Technology (UNIST), Ulsan 44919, Korea; ersgis@unist.ac.kr

* Correspondence: ljquack@esf.edu; Tel.: +1-315-470-4727

Received: 19 July 2020; Accepted: 8 September 2020; Published: 10 September 2020



Abstract: Leaf area index (LAI) is an important vegetation leaf structure parameter in forest and agricultural ecosystems. Remote sensing techniques can provide an effective alternative to field-based observation of LAI. Differences in canopy structure result in different sensor types (active or passive), platforms (terrestrial, airborne, or satellite), and models being appropriate for the LAI estimation of forest and agricultural systems. This study reviews the application of remote sensing-based approaches across different system configurations (passive, active, and multisource sensors on different collection platforms) that are used to estimate forest and crop LAI and explores uncertainty analysis in LAI estimation. A comparison of the difference in LAI estimation for forest and agricultural applications given the different structure of these ecosystems is presented, particularly as this relates to spatial scale. The ease of use of empirical models supports these as the preferred choice for forest and crop LAI estimation. However, performance variation among different empirical models for forest and crop LAI estimation limits the broad application of specific models. The development of models that facilitate the strategic incorporation of local physiology and biochemistry parameters for specific forests and crop growth stages from various temperature zones could improve the accuracy of LAI estimation models and help develop models that can be applied more broadly. In terms of scale issues, both spectral and spatial scales impact the estimation of LAI. Exploration of the quantitative relationship between scales of data from different sensors could help forest and crop managers more appropriately and effectively apply different data sources. Uncertainty coming from various sources results in reduced accuracy in estimating LAI. While Bayesian approaches have proven effective to quantify LAI estimation uncertainty based on the uncertainty of model inputs, there is still a need to quantify uncertainty from remote sensing data source, ground measurements and related environmental factors to mitigate the impacts of model uncertainty and improve LAI estimation.

Keywords: LAI estimation; passive; active; data source; model inversion; scale effect; uncertainty

1. Introduction

Forest and agricultural systems are dominant components of the global ecosystem [1], and understanding how management actions impact their growth patterns [2,3] and their effect on global climate is important [4–6]. Leaf area index (LAI) is one of many biophysical parameters that play a significant role in monitoring plant nutritional and health status and can serve as an indicator of stress and damage [7,8]. Moreover, LAI is an important input to many climate [9,10], ecological [11],

terrestrial primary production [12,13] and crop growth [14] models. Since the 1990s, LAI estimation has been widely studied in forest [15,16] and agricultural [17,18] systems. Breda [19], Jonckheere et al. [20], Weiss et al. [21], Chen [22], and Qu [23] reviewed experiment design, sampling methods, instruments, and estimation theories for ground-based measurements of LAI. Ground LAI measurement methods are generally divided into two major categories: direct and indirect [24]. Direct measurements include destructive sampling and litterfall collection and are more accurate than indirect methods [20]. Indirect measurements include using optical instruments and estimation models [20,25]. Several devices have been created to improve the efficiency of ground-based measurements of LAI [26]. Based on the gap fraction, which describes light penetration and the amount and distribution of openings in the canopy [27], indirect ground measurements quantify effective LAI (eLAI). Effective LAI is a reduction of true LAI based on the clumping index, which characterizes the effect of nonrandom spatial distribution of foliage on LAI measurements [25]. Therefore, eLAI is smaller than true LAI [25]. Yan et al. [26] describe popular methods, recent advances, challenges, and perspectives of indirect optical ground measurement of LAI, and present clumping correction methods to explain the conversion from eLAI to true LAI. However, ground LAI measurements are labor-intensive, time-consuming, and may only be appropriate for small areas and small stature crops rather than the large extents typical of forests and many agricultural applications.

The development of remote sensing techniques has provided powerful and effective tools for estimating the spatial distribution of LAI for large areas and how LAI changes over time [15,16,28,29]. The increased availability of a large number of sensors with diverse spatial, spectral, temporal, and radiometric characteristics has led to consideration of spatial and spectral scale effects becoming a crucial focus for effectively applying remote sensing data [30]. Furthermore, the impact of these scale effects varies from model to model [31] when remote sensing data is used for LAI estimation. Prior studies have explored the field of LAI estimation from remotely sensed data. Baret and Buis [32] described methods and challenges with canopy characteristic estimation from remote sensing observations, and suggested ways to improve retrieval performance, including using prior information, and incorporating spatial or temporal constraints. Zheng and Moskal [27] reviewed inversion theories and methods of LAI estimation from different sensors and concluded that lidar data could provide accurate, timely, and meaningful information to improve LAI estimation. Song [33] reviewed the use of optical remote sensing in mapping LAI and discussed empirical approaches using spectral and spatial information, as well as semi-empirical and biophysical approaches. Song [33] anticipated that new algorithms using complementary information from different sensors would lead to the generation of better global LAI products. Chen [22] presented LAI principles and algorithms and highlighted issues associated with LAI retrieval using remote sensing data, including the differences among existing global LAI products and distorted seasonal variations of LAI. This paper updates and extends these prior studies by exploring recent advances of LAI estimation in forest and agricultural systems. We review and compare different remote sensing-based approaches to estimate LAI from passive and active detection systems. In addition, based on the synthesis of information from 190 papers published over the past three decades, we present the advantages, disadvantages, and research trends in the application of different sensor types and models, discuss scale and uncertainty issues, and propose future directions of LAI estimation to support forest and crop management.

2. Materials and Methods

This study performed a title and key word search using “LAI estimation” or “leaf area index estimation” of the Web of Science and Google Scholar databases with a date limit of 1990–2019. This search yielded 314 results from Web of Science and 590 from the Google Scholar database. These results were filtered to eliminate review papers, conference proceedings, LAI estimated for vegetation cover types not of interest (e.g., grasslands and wetlands), studies focused on LAI application for estimating other parameters, and ground-based LAI estimates from handheld devices. This reduced the dataset to 190 papers from 20 journals (Table 1). Based on the number of published papers, the top

five journals were *Remote Sensing of Environment*, followed by *Remote Sensing*, *International Journal of Remote Sensing*, *IEEE Transactions on Geoscience and Remote Sensing*, and the *International Journal of Applied Earth Observation and Geoinformation*.

Table 1. Journal list and the number of papers (#) for forest and crop LAI estimation from 1990–2019.

Name of Journal	#	Name of Journal	#
Remote Sensing of Environment	51	Computers and Electronics in Agriculture	1
Remote Sensing	28	Ecological Applications	1
International Journal of Remote Sensing	19	Ecological Indicators	1
IEEE Transactions on Geoscience and Remote Sensing	13	Environmental Monitoring and Assessment	1
International Journal of Applied Earth Observation and Geoinformation	10	Estuarine, Coastal and Shelf Science	1
Agricultural and Forest Meteorology	8	European Journal of Agronomy	1
IEEE Journal of Selected Topics in Applied Earth Observations and Remote Sensing	8	Field Crops Research	1
Canadian Journal of Remote Sensing	6	Geophysical Research Letters	1
ISPRS Journal of Photogrammetry and Remote Sensing	6	International Journal of Biometeorology	1
GIScience & Remote Sensing	4	Journal of environmental management	1
Remote Sensing Letters	4	Journal of Forestry Research	1
Forest Ecology and Management	2	Journal of Geography, Environment and Earth Science International	1
Forests	2	Journal of Integrative Agriculture	1
Geocarto International	2	Journal of Quantitative Spectroscopy and Radiative Transfer	1
Journal of Geophysical Research: Biogeosciences	2	Journal of Remote Sensing	1
Annals of Forest Science	1	Journal of Sustainable Forestry	1
Aquatic Botany	1	Plant Methods	1
Boreal Environment Research	1	Precision Agriculture	1
Chinese Journal of Geophysics	1	Sensors	1
Chinese Science Bulletin	1	Silva Fennica	1

3. Remote Sensing Data Sources and Limitations

3.1. Trends in Data Applied to Estimating Forest and Crop LAI

This paper reviews 225 studies (in 190 papers, where 32 papers examined multiple data sources with a single model) from the past three decades that focused on LAI estimation; of these about 60% related to forests and 40% to crops (Table 2). A full list of the papers used to generate the data in Table 2 is provided in Supplementary Table S1. The full list also presents whether each paper used true LAI or eLAI ground data sources. Where there was no description regarding correction from eLAI to LAI, we assumed the measurement was eLAI. Of the 190 papers, 178 used optical-based devices to quantify eLAI to generate data for model building and model validation (Supplementary Table S1). Only 12 papers quantified true LAI using direct methods.

Table 2. Summary of the application of types of different detection systems and platforms used to estimate LAI in forest and crops from 1990–2019.

Detection System	Platform	Number of Studies		Advantages	Disadvantages
		Forest	Crop		
Passive remote sensing	Airborne	Manned	13	7	Suitable for forests and crops, including complex vegetation types and structures
		Unmanned	2	9	Optimum spatial and spectral data resolution with quick turnaround times that supports real-time crop management
		Satellite	70	54	Better for multi-temporal analysis, especially for large extents
	Total	85	70		Limited access to high spatial and spectral resolution data
	Terrestrial	Lidar	13	3	Provides three-dimensional distribution of plant canopies at individual tree or stand levels
Active remote sensing	Airborne	Lidar	17	3	Provide information about canopy structure
		Radar	0	2	
	Satellite	Lidar	3	0	Provide information about canopy structure over large extents
		Radar	3	5	Provide information about canopy structure over large extents; avoid cloud issues
	Total	36	13		Complicated data processing; limited availability of data
Multi-source		9	12	Combine advantages of multiple data sources	No general methods to integrate data sources
Grand Total		130	95		

Remote sensing devices are fundamentally divided into two categories: passive and active detection systems. Both types have more applications to forest systems in terms of the number of published LAI-focused studies. Table 2 summarizes the number of studies and the key advantages and disadvantages in the application and use (e.g., access to data, data processing, and types of products generated) of different sensor types for forest and crop LAI estimation that were reported in the literature over the past three decades. Passive remote sensing data sources are the most widely used source for LAI estimation in both forest and agricultural systems, with smaller proportions of studies using active and multisource remote sensing. This review shows that the number of LAI estimation studies using passive remote sensing increased from the 1990s to 2010s for both forest (11–42 studies) and crop (1–48 studies) applications (Figure 1). This trend also occurred for active remote sensing from the 1990s to 2010s for both forest (0–28 studies) and crop (1–12 studies) applications (Figure 1, Table S1). Similarly, forest and crop LAI estimation applications of multiple data source remote sensing also showed an increasing trend from 1990 to 2019.

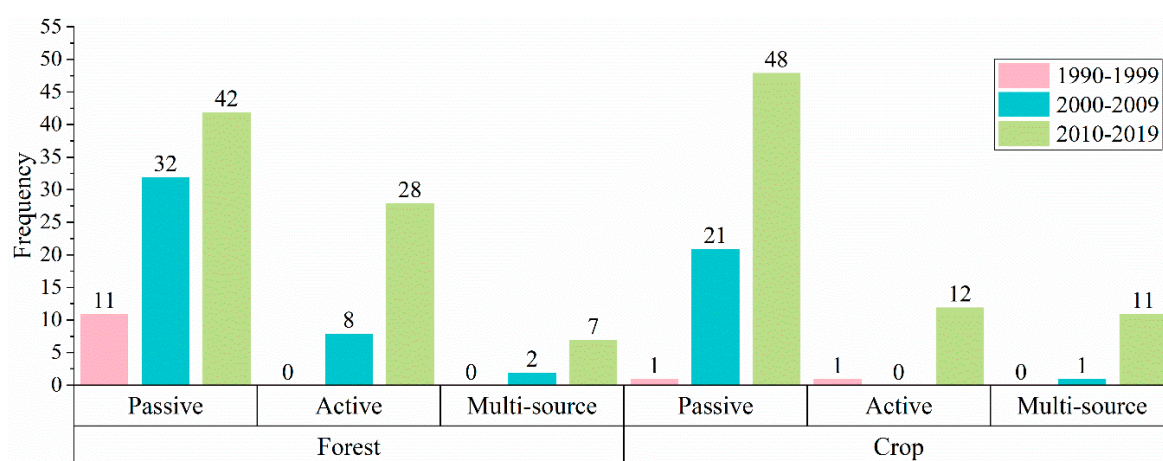


Figure 1. Temporal trends of the application of different detection systems for forest and crop LAI estimation from 1990–2019.

In general, agricultural systems are more homogeneous and more easily accessible than forest systems. High accessibility in particular tends to support application of unmanned airborne passive data for crop LAI estimation, while the complicated vegetation types in forests have more frequently been observed using manned airborne passive data. The number of passive satellite data sources that are now freely available have supported wide use in both forest and crop LAI estimation. Of the 225 studies cited in this paper, the number of forest and crop LAI estimation studies using passive remote sensing is almost three times as many as active remote sensing studies. In terms of active remote sensing, lidar data are more widely used for forest systems than for agricultural systems. Lidar can detect complex forest canopy structure, which facilitates observation of significant parameters and researchers have sought ways to use lidar data to improve forest LAI estimation through improving modeling [34] and mitigating the impact of saturation [35]. Radar systems have also been used for both forest and crop LAI estimation. Since agricultural systems are very dynamic throughout the growing season and vary from field to field or even within individual fields [36], radar systems that mitigate cloud concerns are useful for crop LAI estimation, especially for time-series crop monitoring analysis. However, the large extent of many forests creates challenges associated with obtaining and processing radar data, which currently limits their use to estimate forest LAI.

3.2. Passive Remote Sensing

This section describes the application of airborne and space-based spectroscopy from passive remote sensing devices to support LAI measurement, including hyperspectral and multispectral data. The different platforms vary in applicability to support different forest and agricultural system usage.

Manned and unmanned airborne system (UAS) data have been applied for both forest and crop LAI estimation. Forests are often managed or monitored over larger areas than crops, and thus there are practical limits in the application of airborne-based remote sensing for forest LAI estimation, particularly if multi-temporal analysis is required. Due to improvement in unmanned aerial vehicles (UAV), sensors, and UAS data processing software (e.g., the very popular Pix4D mapper [37]) over the last 10 years, the UAS platform facilitates optimum spatial and spectral data resolution with quick turnaround times that support real-time crop management. Zhang and Kovacs [38] discussed the advantages of using UAS-based sensors with ultra-high spatial resolution (e.g., centimeters) and relatively low operational costs for LAI estimation. Roosjen et al. [39] generated potato LAI from UAS data with $R^2 = 0.91$ and RMSE = 0.70, which showed good potential for LAI estimation from UAS data. Tian et al. [40] evaluated mapping mangrove forest LAI using a UAS-based multispectral sensor (6 bands with 1 cm pixel size) and WorldView-2 imagery (WV2, 8 bands, 1.8 m). Their results showed that the UAS-based system (coefficient of determination (R^2) = 0.82, root mean square error (RMSE) = 0.42) performed better than WV2 imagery ($R^2 = 0.78$, RMSE = 0.42) in areas with homogeneous mangrove species, but the WV2 imagery performed better than the UAS-based data for sites with a variety of mangrove species. Based on the summary of studies reported in Supplementary Table S1, all of the UAS-based LAI applications reported were in the past 10 years, with approximately 70% focused on crop LAI estimation. Uniformity of background and vegetation types appear to be two critical factors constraining the application of UAS data for forest LAI estimation. Forests tend to be more complex with variability in vegetation type and structure, while crops often have more uniform characteristics with a singular vegetation type and homogeneous background [40,41]. However, the continued development of UAS platform hardware will likely improve forest and crop LAI estimation and enhance forest and agricultural management.

Since the launch of the first Landsat satellite in the early 1970s, the field of space-borne optical remote sensing has made significant progress [42]. Free data sources such as the various Landsat and Sentinel sensors, as well as lower spatial resolution Moderate Resolution Imaging Spectroradiometer (MODIS) and Medium Resolution Imaging Spectrometer (MERIS) data have been more popular for forest and crop LAI estimation than commercial satellites such as QuickBird, IKONOS and SPOT. Radiometric, geometric, and atmospheric corrections that are now applied to available Landsat and Sentinel data reduce the time associated with data preprocessing but also makes these passive satellite data sources more easily and consistently used [43,44]. Currently, the Landsat Collection 2 includes Landsat Level-1 data for all sensors since 1972 and global Level-2 surface reflectance since mid-2020, which can be downloaded from the United States Geological Survey Earth Explorer (<https://earthexplorer.usgs.gov/>). Level-2A Sentinel-2 data are available for download from the European Space Agency Copernicus Open Access Hub (<https://scihub.copernicus.eu/dhus/#/home>).

Researchers have used remotely sensed data to estimate LAI across a range of scales (noted in Supplementary Table S1). While the majority of studies (178) focused on local scale analysis, research was also conducted at regional (five studies) and global (seven studies) scales. MODIS, MERIS, and other coarse data have particular application for generating global LAI products because the data choice is often based on the study area extent. The high temporal resolution of these datasets also helps detect global LAI changes based on time-series images. Campos-Taberner et al. [45] provided a quantitative assessment of the quality of MODIS (MOD15A2), Copernicus PROBA-V (GEOV1), and the recent EUMETSAT Polar System (EPS) LAI products for rice LAI estimation and concluded that these three products were closely related to LAI estimates from Sentinel-2 and Landsat 7/8 ($R^2 \approx 0.90$, RMSE ≈ 0.50). Fang et al. [46] provide an overview of the methods, validation, and applications of global LAI products. They concluded that new algorithms are needed to advance LAI estimation and also expressed a need to address the inadequacy of current validation studies. MODIS (250 m–1 km) and MERIS (300 m) data are not widely used for precision agriculture research, particularly for small study sites, because the spatial resolution is often too coarse for such applications.

3.3. Active Remote Sensing

Active remote sensing has two common systems: radio detection and ranging (radar) and light detection and ranging (lidar). Both radar and lidar systems can detect canopy structure because the range response captured generates both horizontal and vertical information [27,47,48]. Based on the atmospheric window within the microwave portion of the spectrum [49], radar systems emit long wavelength electromagnetic energy and identify the range to the target by capturing reflected waves [27]. Lidar systems are based on an application of light amplification by stimulated emission of radiation (laser) [50] and actively emit shorter wavelength energy (such as green or near infrared wavelengths). This section discusses the application of active remote sensing to forest and crop LAI estimation from terrestrial, airborne, and satellite platforms.

Active terrestrial remote sensing applications in LAI estimation are primarily limited to lidar systems. Terrestrial lidar provides three-dimensional (3D) distribution of plant canopies at individual tree or stand levels and has been widely used for quantifying vegetation LAI through direct measurements of gap fraction with R^2 up to 0.98 [51–54]. Although terrestrial lidar can deliver the finest characteristics of forest structure, including tree trunks, branches, twigs, and leaves, it is difficult to fully recover all the tree components because of occlusion from nearer-range vegetative elements [55,56], which may limit broad application.

Numerous researchers have applied airborne lidar data for forest LAI estimation (e.g., [57–60]). However, there are fewer applications reported in agricultural systems. This may be because discrete lidar data tend to have poor penetration ability in short, and dense vegetation [61–63]. Previous studies have also proposed derivation of LAI from airborne radar data. Hosseini et al. [64] successfully used different L-band polarizations of a UAS-mounted synthetic aperture radar (SAR) to estimate LAI for corn canopies ($R^2 = 0.58\text{--}0.86$) but their analysis failed for soybean ($R^2 = 0\text{--}0.14$). Hosseini et al. [64] suggested that L-band data may be more suitable for larger canopies in both horizontal and vertical dimensions, a conclusion that was consistent with another study performed by Paloscia [65]. While these examples show some applications for estimating crop LAI using airborne radar data, applications of this data for forest LAI estimation are more limited and the suitability of airborne radar data for both forest and crop LAI estimation needs further research.

The Geoscience Laser Altimeter System (GLAS), a satellite-based laser altimeter and lidar sensor on the Earth Observing System (EOS) ICESat mission [66] that operated from January 2003 to August 2010 proved useful for vegetation-focused analysis. Tang et al. [67] used ICESat data in a study to estimate LAI over conifer-dominated forests and validated the application of GLAS as an accurate standalone LAI sensor ($R^2 = 0.84$, RMSE = 0.33). Compared to forest applications, the complexity of data processing, the limited availability of data, and the rapid changes in LAI over short time periods appear to have hindered research in crop LAI estimation from satellite-based lidar data. The follow-on to the ICESat mission, ICESat-2, was launched on September 2018 and carries the Advanced Topographic Laser Altimeter System (ATLAS). This sensor is expected to provide vegetation canopy information (<https://www.nasa.gov/content/goddard/icesat-2-technical-requirements/>) that will have value for LAI estimation.

Satellite-based radar data are less influenced by the atmosphere [64] and are more widely used for LAI estimation than satellite-based lidar data. Inoue et al. [68] found rice paddy LAI was closely related ($R^2 = 0.84$) to C-band backscattering coefficients from the Radarsat-2 sensor but suggested that the limited spatial resolution of early SAR sensors led to low accuracy and inconsistency, which limited operational applications to LAI estimation. Difficulties associated with data processing and acquisition have historically limited wide application of radar for forest and crop LAI estimation. With improvements in resolution and access, the distinct advantages of satellite-based radar systems to provide forest and crop information under cloudy weather conditions may be more readily harnessed, which will likely lead to improved forest and crop LAI estimation.

3.4. Multi-Source Remote Sensing

As described above, individual remote sensing data have distinct advantages and disadvantages for forest and crop LAI estimation. A common approach applied to mitigate the limitations of single-sensor analysis is fusion of spatial, spectral, or temporal information from multiple sensors [69]. For example, Gray and Song [69] developed a method to use spectral information from Landsat (8 bands, 30 m), spatial information from IKONOS (1–4 m), and temporal information from MODIS (daily, 250 m) in order to generate maps of forest LAI ($R^2 = 0.73$) at Landsat spatial resolution (30 m) with daily temporal resolution. This combination of spatial and temporal resolutions cannot be accomplished through single sensor analysis. Chai et al. [70] fused different LAI products, including SPOT VEGETATION LAI and MODIS LAI products to offset the limitation caused by spatial or temporal discontinuities in LAI derived from a single data source, successfully generating spatially continuous LAI estimates for different vegetation types ($R^2 \approx 0.9$ and RMSE ≈ 0.3). The combination of active and passive data can also be used for LAI estimation ($R^2 = 0.68$) [71], and this approach has been applied to both forest and agricultural systems. Gao et al. [72] proposed a modified vegetation index (VI) to estimate maize LAI using both multispectral remote sensing data from the HJ-1 small-sat and HV cross-polarization of RADARSAT-2 data in order to overcome saturation limitations from optical VIs, which increased R^2 from 0.25 to 0.52. Yang et al. [73] found ~65 m ICESat/GLAS full waveform data often included discontinuous forest patches but combining these data with Landsat images that provided crown coverage information within the GLAS footprint improved forest LAI estimation ($R^2 = 0.83$, RMSE = 0.39).

4. LAI Estimation Models

4.1. Trends in Models Applied to Estimating Forest and Crop LAI

LAI estimation models mainly fall into three categories: empirical, physical, and hybrid models [74]. Empirical models seek to establish a relationship between LAI and spectral reflectance or some transformation of reflectance, e.g., VIs, using regression methods [75]. Physical models are based on radiative transfer theory, which accounts for the interaction of electromagnetic radiation with plant leaves associated with various biophysical and biochemical parameters [76]. Hybrid models estimate LAI based on simulated spectra from physical models. All three model types are widely used for LAI estimation using remote sensing data sources.

Table 3 lists the number of studies focused on forest and crop LAI estimation using empirical, physical, hybrid, and other models, provides the accuracy range and one recent example for each category, and summarizes the methods used in these models over the past three decades. Model performance was quantified by R^2 and RMSE, though the majority of the studies did not perform any independent validation. Of the 190 papers, eight performed validation using independent datasets and forty-eight papers used classical cross validation methods (e.g., leave-one-out [77], k-fold [78], and hold-out [70] methods) that divide a dataset repeatedly into training, validation, and testing parts. Based on the conclusions reported in these studies, where possible, we recommend maximizing the range of LAI values in the field data collected to enhance model robustness. We also recommend conducting validation using independent data where possible. However, given the frequent challenges in data access, if independent data is not available, cross validation has value to evaluate model overfitting. The total number of estimation models reported in Table 3 (227) is higher than the number of papers reviewed because 29 papers examined multiple models with a single data source. A full list of the papers used to generate the data in Table 3 is provided in the Supplementary Table S2. There has been a dramatic increase in the number of studies exploring different models for forest and crop LAI estimation each decade over the past 30 years, particularly in exploration of new VIs and models. Empirical models are the most widely used for LAI estimation in both forest (67%) and agricultural (56%) systems (Figure 2). The percentage of empirical models for forest LAI estimation is higher than for crops while the percentage of physical, especially PROSPECT+SAIL (PROSAIL) and hybrid, models

for forest LAI estimation is lower than that for crops. These differences may reflect the relatively smaller individual management area of agricultural systems as well as the more complicated structure of forest systems. Figure 3 shows the temporal trends of the number of papers that applied each type of model for estimating forest and crop LAI. As can be seen in this figure, there is a trend of increasing applications of all model types, with the greatest growth being the application of empirical models for crop LAI estimation, where the number of studies during the past decade is six times greater than during the 2000s.

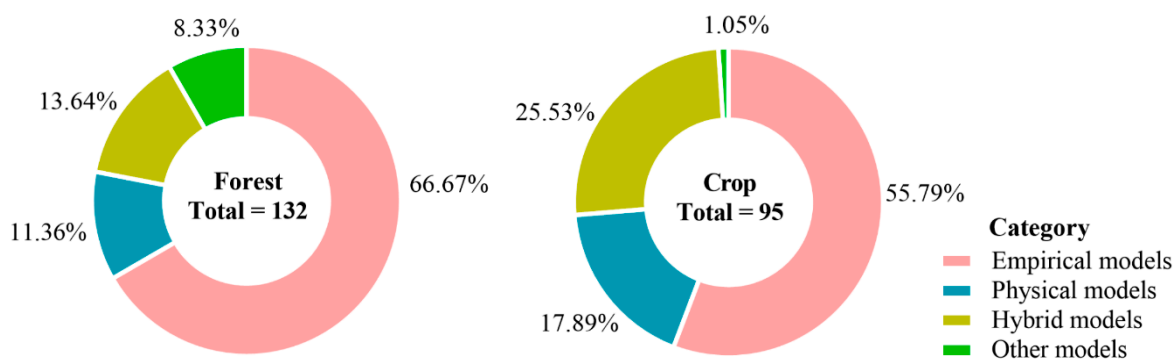


Figure 2. Distribution of different model types for forest (left) and crop (right) LAI estimation.

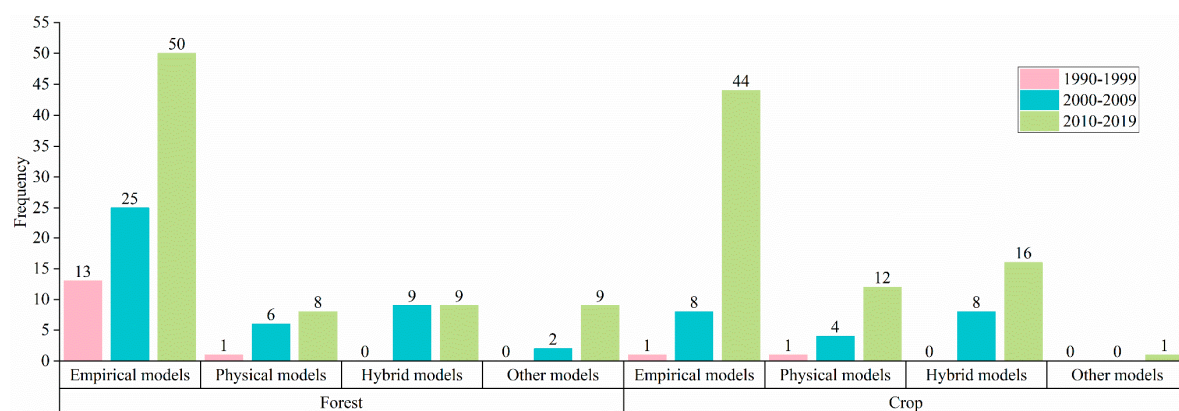


Figure 3. Temporal trends of number of papers published with four different model types for forest and crop LAI estimation from 1990–2019.

Table 3. Summary of models and model performance for forest and crop LAI estimation reported from 1990–2019.

Model	Sensors	Forest				Crop				Algorithms
		N	R ²	RMSE	Examples	N	R ²	RMSE	Examples	
Empirical Models	Reflectance-based	13	0.59–0.97	0.10–1.08	Korhonen et al. [79]	7	0.59–0.82	0.53–1.52	Li et al. [80]	Regression
	VI-based	39	0.14–0.97	0.05–2.41	Meyer et al. [81]	31	0.45–0.95	0.02–1.81	Qiao et al. [82]	Wide range of VIs
	Derived metrics	29	0.58–0.98	0.01–1.46	Zhang et al. [83]	3	0.36–0.95	0.16–0.45	Li et al. [84]	Regression
	Machine learning models	7	0.85–0.93	0.48–1.94	Neinavaz et al. [85]	12	0.58–0.97	0.1–1.94	Lin et al. [86]	ML algorithms
	Total	88	0.14–0.98	0.01–2.41		53	0.36–0.97	0.02–1.94		
Physical (radiative transfer) Models	DART	2	0.60–0.72	0.50–1.20	Banskota et al. [87]	0				look-up tables (LUTs)
	4-Scale bidirectional reflectance distribution (BRD)	2	0.80–0.85	0.79–1.30	Liu et al. [88]	1	0.85	1.30	Deng et al. [89]	
	PROSPECT+DART	1	0.77	0.46	Banskota et al. [90]	0				Iterative optimization, LUTs
	PROSAIL	2	0.80	0.41–0.47	Le Maire et al. [91]	11	0.82–0.99	0.13–1.48	Su et al. [92]	
	Other models	8	0.72–0.95	0.82–0.93	Ma et al. [93]	5	0.83	0.34–0.93	Liu et al. [94]	LUTs, dynamic model, etc.
Hybrid Models	Total	15	0.60–0.95	0.41–1.3		17	0.83–0.99	0.14–1.94		
	Empirical+	4-Scale BRD	2	0.42–0.59	0.30–1.08	Gonsamo and Chen [95]	2	0.42–0.59	0.3–1.08	Gonsamo and Chen [95]
		PARAS	3	0.71–0.85	0.48–0.52	Varvia et al. [96]	0			
		PROSAIL	6	0.64–0.91	0.27–1.15	Xing et al. [97]	15	0.62–0.96	0.3–1.15	Xu et al. [98]
		Other models	7	0.20–0.99	0.20–1.85	Shi et al. [99]	7	0.58–0.94	0.01–1	Qu et al. [100]
	Total	18	0.20–0.99	0.20–1.85		24	0.42–0.96	0.01–1.15		
Other Models	Wang et al. [101]	11	0.49–0.96	0.01–0.90		1		0.50	Liu et al. [102]	Regional phenology model, path length distribution model, etc.
	Grand Total	132	0.14–0.99	0.01–2.41		95	0.36–0.99	0.01–1.94		

4.2. Empirical Models

The empirical models most commonly used to estimate LAI use spectral reflectance-based parameters [103], vegetation indices [104], derived metrics, and machine learning methods. The R^2 range of empirical models is 0.14–0.98 and the RMSE range is 0.01–2.41, which indicate the variable performance of different empirical models (Table 3). In terms of R^2 , machine learning methods provide relatively consistent performance (0.85–0.93). Simple reflectance-based models utilize ordinary regression or partial least square regression to establish the relationship between spectral reflectance and LAI [105]. Korhonen et al. [79] found the Sentinel-2 red-edge band ($R^2 \approx 0.70$) and the Landsat TM green band ($R^2 \approx 0.70$) were closely related to boreal forest LAI based on regression analysis. Several studies have also used regression approaches to demonstrate the relationship between radar data from airborne- and satellite-based platform and LAI [64,65,106]. Vegetation indices are another commonly used input for estimating LAI using an empirical approach. VIs combine surface reflectance from multiple bands and are designed to maximize information about canopy characteristics and minimize interference factors from the atmosphere and soil [94]. Kross et al. [107] compared the ability of seven VIs to estimate corn and soybean LAI using RapidEye data and demonstrated the instability and variable sensitivities of using VI-based methods for LAI estimation. It appears that no VI can be applied generally: specific indices are needed for specific regions and crop types.

Derived metrics-based models are frequently applied to lidar data. Such models utilize regression techniques to estimate LAI from calculated metrics such as canopy height, cover metrics, height distribution metrics, penetration rate, number of ground returns, total returns, and texture information [60,108]. Solberg et al. [109] found penetration rate calculated from airborne lidar data was closely related to LAI ($R^2 > 0.9$). Wulder et al. [110] related NDVI from CASI images to conifer and deciduous forest LAI, and found that R^2 value increased from 0.67 to 0.92 when texture information was added. Similarly, for mixed forest stands, the addition of texture information increased R^2 value between NDVI and LAI from 0.01 to 0.44 [111].

Within the different types of models, the rapid development of machine learning methods has influenced the algorithms utilized for estimating forest and crop LAI. Machine learning models are often used in empirical approaches to explore optimal models based on experiments using training, validation and test datasets [112]. The most popular methods include artificial neural networks (ANNs), Gaussian processes regression (GPR), Bayes algorithm, support vector regression (SVR), and random forest (RF) regression. Verrelst et al. [112] compared four machine learning regression algorithms (ANN, SVR, kernel ridge regression (KRR), and GPR) using Sentinel-2 and -3 data for estimating biophysical parameter retrieval and concluded that GPR had the best performance (relative RMSE ≈ 0.2) when compared to the other three methods. Wang et al. [113] used a neural network approach to combine HJ-1 CCD, GF-1, Landsat TM, Landsat Enhanced Thematic Mapper Plus (ETM+), and MODIS data, which enabled them to fill in missing data in the Landsat images in order to generate continuous time series (8 days) crop LAI with 30 m resolution (RMSE = 0.30).

4.3. Physical (Radiative Transfer) Models

In contrast to empirical models, physical models based on physical principles of radiative transfer are run in forward mode to simulate reflectance and transmittance with the input of vegetation biophysical and biochemical parameters and other related environmental parameters [114]. In terms of R^2 (0.60–0.95) and RMSE (0.41–1.3) range, physical models provide more consistent performance than empirical models (Table 3). Researchers have explored physical models at both leaf and canopy levels. Table 4 summarizes some of the key forward physical models that are discussed further in this section. Other models that are less frequently reported in the literature include the Geometric Optical Mutual Shadowing (GOMS) model [115,116], Kuusk–Nilson forest reflectance model [117,118], Geometric Optical and Radiative Transfer (GORT) model [119,120], and a two-layer canopy-reflectance model (ACRM) [94,121]. DART is a 3D canopy reflectance model developed by Gastellu-Etchegorry et al. [122] and supports consideration of vertical information. The 4-Scale BRD model is a forest-specific physical

model so named because it considers four-scales: tree groups, tree crowns, branches, and shoots. PARAS is another forest reflectance model used to estimate LAI that takes into account the effect of within-shoot scattering on coniferous canopy reflectance.

Table 4. Summary of popular physical models for characterizing LAI.

Model	Name Origin	Application	Reference
DART	Discrete anisotropic radiative transfer	Forest/crop	Gastellu-Etchegorry et al. [122]
PROSPECT+DART	PROSPECT+DART	Forest/crop	Banskota et al. [90]
4-Scale BRD	Four-scale bidirectional reflectance model	Forest	Chen and Leblanc [123]
PARAS	Parameterization model	Forest	Rautiainen and Stenberg [124]
PROSAIL	PROSPECT+SAIL	Forest/crop	Verhoef [125]; Jacquemoud and Baret [76]; Jacquemoud et al. [114]

Some studies have combined leaf and canopy models to simulate canopy reflectance in order to account for light transmission influenced by various canopy physiological and biochemistry parameters [39,126]. The PROSAIL model merges the PROSPECT leaf optical properties model and the SAIL canopy bidirectional reflectance model. Due to its ease of use, general robustness, and consistent results, the PROSAIL model has become a particularly popular radiative transfer tools [114]. In addition, the model is open-source, which makes it easier for people to utilize and explore new methods. Mananze et al. [127] estimated maize LAI using the PROSAIL model and found PROSAIL led to satisfactory accuracy ($\text{RMSE} \approx 0.2$) while overcoming the reliance on field measurements inherent in developing VI-based empirical models.

Another relatively new combined approach uses the PROSPECT and DART models. Following a similar framework as the PROSAIL model, this new approach uses PROSPECT for calculating leaf hemispherical reflectance and transmittance and combines this with DART parameters (LAI, leaf angle distribution, soil reflectance, and crown cover) to simulate canopy reflectance and transmittance. As mentioned in Section 4.3, the vertical information provided by DART could help improve crop LAI information. Therefore, the use of the combined PROSPECT and DART model for estimating forest and crop LAI should be explored in future research.

Several inversion algorithms have been applied based on the forward mode of physical models [128]. These include numerical optimization and look-up tables (LUTs). Iterative optimization is a classic technique to invert physical models. Iterative optimization aims to create an optimal solution by minimizing a merit function that estimates the difference between measured and estimated variables in successive iterations [128]. However, the time-consuming nature of the process, especially for complex physical models, constrains its application [129]. LUTs generate a training table with forward radiative transfer models for a discrete set of input variables covering their prescribed range of variation [114]. The use of an LUT involves minimization of a merit function that minimizes the summed differences between simulated and measured reflectance for all wavelengths. LUTs are used extensively to speed up the inversion process because they can pre-define model reflectance for a large number of combinations of parameter values [130], but the process of searching for the optimal solution for complex models is time-consuming.

4.4. Hybrid Models

An alternative to using empirical or physical models alone are hybrid models that combine the two techniques. Combining the two fundamental approaches takes advantage of the generic properties of physical-based methods and the flexibility and computational efficiency of empirical methods including various VIs and machine learning models [112,131–134]. Physical models are used

for simulating spectra dataset based on the input of various vegetation biophysical and biochemical parameters. Compared with empirical and physical models, hybrid models provide a compromise in performance (R^2 range is 0.20–0.99 and RMSE range is 0.01–1.85, Table 3). Hybrid models could be utilized to analyze the performance of VIs, help calibrate traditional VIs [91], and create new VIs based on running forward physical models with specific data sources. Chaurasia and Dadhwal [131] demonstrated that a multi-band principal component inversion (PCI) approach based on the PROSAIL model performed better (RMSE = 0.38) for crop LAI estimation than empirical models based on NDVI (RMSE = 2.28) and SR (RMSE = 0.88). In terms of machine learning methods, ANNs are the most prevalent in the literature related to LAI estimation. ANNs mimic the way that information is processed in the brain through a network of interconnected neurons [135,136]. Previous research has reported that ANNs can estimate biophysical variables more accurately than empirical methods [103]. ANNs have been applied to LAI estimation at a variety of scales, from local or regional projects up to global products, such as that produced by Baret et al. [137]. Xu et al. [98] estimated rice LAI using a Bayesian network and the cost function method based on the PROSAIL model. Their results indicated that the Bayesian network provided better performance ($R^2 = 0.81$) than the cost function method ($R^2 = 0.51$). Hybrid models take advantage of the strengths of both empirical and physical models. The practical challenge in applying this knowledge is that the optimal VIs identified based on the physical model may not have corresponding bands in the remote sensing data due to the limited spectral resolution of the most commonly available datasets.

5. Scale Effect

Lam and Quattrochi [138] describe scale from three perspectives: spatial, temporal, and spatiotemporal. Complicating this further, the development of remote sensing technology has led to additional considerations since remote sensing devices also vary in terms of spectral, temporal, and radiometric characteristics. This review focuses on spectral and spatial scale effects, which have been reported as being significant in remote sensing-based LAI observation. Radiometric resolution, which refers to sensitivity in terms of reflectance levels, of many sensor systems, such as those on the Landsat missions, has increased over time. Additionally, since high-radiometric-resolution data may not be critical for LAI estimation [139], this study does not provide more details about radiometric resolution issues. There is often a tradeoff between spatial resolution and temporal resolution. High-temporal remote sensing images could provide more information for monitoring seasonal dynamic changes in LAI. However, few LAI-focused studies specifically reported temporal scale impacts and this may be an area for future analysis.

5.1. Spectral Scale Effect

Remote sensing devices can be divided based on spectral characteristics, e.g., hyperspectral versus multispectral observation capability. Most hyperspectral data are acquired from airborne platforms, e.g., CASI and AVIRIS [140,141], which have limited capacity over large spatial extents. There have been some satellite-based hyperspectral sensors, such as Earth Observing 1 (EO-1) Hyperion [142,143] and TianGong-1 on the Shenzhou-8 satellite [144], but there are limited available data—both temporally and spatially—from these systems. Pu et al. [142] demonstrated that the Hyperion sensor outperformed two multispectral sensors (Advanced Land Imager and Landsat ETM+) for coniferous forest LAI estimation. For their study area, Pu et al. [142] found that the most important bands were in the shortwave infrared (SWIR) region. Relationships between tropical rainforest LAI and spectral reflectance near the red edge region ($R^2 = 0.67$, RMSE = 0.72) and most SWIR bands ($R^2 = 0.72$, RMSE = 0.60) from Hyperion data were also observed by Twele et al. [145]. Gong et al. [146] concluded that in addition to SWIR response, the NIR region is also important for estimating LAI. They also found that narrow band indices performed better than broadband indices. Lee et al. [141] compared AVIRIS data with ETM+ and MODIS data for crop LAI estimation using a regression model. Their results indicated that the number of bands appeared to be the most important advantage for AVIRIS data

producing the best estimation model, containing 23 bands, which had an R^2 of 0.88. Compared with multispectral data, the narrower bandwidth of hyperspectral data provides more detailed spectral information for improving LAI estimation, especially in the red edge, NIR, and SWIR regions. However, Lee et al. [141] also expressed some concern that their model may be overfitting. The development of UAV hyperspectral sensors also show potential to improve LAI estimation [105,147]. However, the relatively higher cost of hyperspectral sensors has likely hindered application for forest and crop LAI estimation. While numerous studies have illustrated that spectral sampling is important for LAI estimation, there have not been any studies published that focus on quantifying these spectral effects for different sensors. This may be a valuable area for further research, but one of the challenges in developing such an analysis is the limited access to hyperspectral data.

5.2. Spatial Scale Effect

Thenkabail [148] divided data into five spatial resolution classes—0.5–4.9 m, 5.0–9.9 m, 10.0–39.9 m, 40.0–249.9 m, and 250 m–1.5 km—that serve as a convenient characterization for discussion. A pixel obtained from a higher resolution sensor is likely to cover relatively homogeneous land cover, whereas a pixel in a lower resolution image may cover a wide range of land cover types and be very heterogeneous [31]. This difference in spatial heterogeneity is the primary driver of the spatial scale effects that can influence LAI estimation accuracy and LAI validation [149]. However, spatial heterogeneity is not only dependent on differences in spatial resolution [150], but also varies with plant canopy size [151], canopy heterogeneity [152], and topography [153]. Friedl et al. [154] found that compared to Landsat TM data, LAI calculated from NDVI derived from lower resolution advanced very high resolution radiometer (AVHRR) reflectance data tended to slightly underestimate (~15%) LAI values. Chen et al. [155] showed that LAI estimated from coarser resolution pixels had errors as high as 25–50%, which they attributed to surface heterogeneity. Tian et al. [156] and Liu et al. [88] showed that LAI is always underestimated when derived from MODIS data and the magnitude of underestimation increased as heterogeneity increased. Spatial scale effects also cause issues during the validation of LAI estimates [157]. The challenge is that the scale of ground LAI measurements is generally different from the spatial resolution of remotely sensed imagery [158]. The Validation of Land European Remote sensing Instruments (VALERI) project proposed a two-step sampling strategy for validation of global products that relates high spatial resolution products to lower resolution products in order to obtain a validation map for the LAI derived from coarse-scale satellite images [159]. Xu et al. [160] proposed an approach (Grading and Upscaling of Ground Measurements, GUGM) that resolves the scale-mismatch issue and maximizes the utility of time-series of site-based LAI measurements.

The demand for up-scaling (moving from a fine to a coarser scale) and down-scaling (from coarse to finer scale) has driven exploration of scale transformation methods to predict the scale at which data are desired [161,162]. Some studies have explored the relationship between products derived using empirical models based on inputs with different spatial resolution [74,88,163,164]. However, these models use a large amount of sample data and lack a clear theoretical interpretation. Physical models, e.g., mathematical and biophysical mechanism-based models, tend to be better for exploring scale analysis because of their robustness. Fractal theory, which includes the property of self-similarity meaning that any part of the feature is statistically indistinguishable from the feature as a whole [165], is also used for scale transformation. Wu et al. [149] developed an LAI scaling transfer model based on fractal theory that performed well in estimating LAI values from different spatial resolution pixels with a maximum RMSE of 0.278. Fractal theory does provide a direction to further explore scale transformation. However, due to variation in the optical parameters of different satellites and different LAI estimation models, the parameter normalization of scaling transfer models still needs further exploration [149].

A large number of studies have analyzed spatial scale effects and many of these studies show that for similar vegetation types, LAI estimated from imagery with similar spatial resolution characteristics provides similar LAI estimation results. Soudani et al. [166] calculated LAI for temperate coniferous

and deciduous forest from IKONOS, SPOT, and ETM+ data and these three data inputs showed similar predictive ability with an uncertainty (RMSE) of about 1.0. The performance of Landsat TM (30 m) and SPOT5 (10 m) data for rice LAI estimation based on the PROSAIL physical model also demonstrated strong correlations ($R^2 > 0.92$) by Campos-Taberner et al. [74]. However, as spatial resolution changes, so too do the estimated LAI values. For example, Fernandes et al. [163] concluded that there was a poor correspondence between spatial patterns of LAI derived from the CASI (2 m) datasets and from the Landsat (30 m) imagery across the varying scales.

Table 5 summarizes the performance of single satellite-based passive remote sensing data sources with different pixel size for forest and crop LAI estimation. Of the 150 studies, about 60% were related to forest LAI estimation and 40% to crop LAI estimation. One recent example is provided for each image source. Since we did not find studies that used data with pixel size of 40.0–249.9 m, this range was not included. The results presented in the literature suggest that we cannot simply conclude that finer spatial resolution is better than coarser resolution data. Based on the range of R^2 values in Table 5 for forest and crop LAI estimation, finer spatial resolutions tended to generate more consistent forest LAI estimates than coarser resolution data. Similarly, crop LAI estimation tended to have smaller R^2 ranges across all pixel sizes compared to forest systems. This is likely tied to the fact that LAI varies with species and land cover tends to be more complicated in forest systems than in agricultural systems [20]. Supplementary Table S1 lists the forest type for the 123 forest-focused papers in this review. For boreal coniferous forests, Schulze [167] reported LAI values ranging from 3 to 19, with the highest values being reported for *Pseudotsuga menziesii*, but a later study of *P. menziesii* reported a 95% confidence interval for LAI estimates of ~7–11 with variability across years [168]. The observed maxima of LAI value for deciduous canopies are typically 6–8, compared to LAI values of 2–4 for crops [169]. The scale effect appears to play a more important role for forest LAI estimation as compared to agricultural applications. The R^2 range (0.14–0.96) of forest LAI estimation studies using data sources with 0.5 m–1.5 km pixel size is wider than crop LAI estimation (0.45 to 0.98), which is likely related to the impact of the greater pixel heterogeneity typical in forests.

Table 5. The performance of single satellite-based passive remote sensing data sources with different pixel size for forest and crop LAI estimation.

Pixel Size	Sensors	Forest				Crop			
		N	R ²	RMSE	Examples	N	R ²	RMSE	Examples
0.5–4.9 m	IKONOS	5	0.58–0.73	1.19	Soudani et al. [166]	1	0.62	N/A	Colombo et al. [170]
	QuickBird	1	0.84	0.41	Zhou et al. [171]	1	0.78	0.08	Wu et al. [172]
	World-View-2	3	0.75–0.78	0.05–0.42	Tian et al. [40]	0			
	Total	9	0.58–0.78	0.05–1.19		2	0.62–0.78	0.08	
5.0–9.9 m	ZY-3	1	0.74	0.57	Wang et al. [101]	0			
	RapidEye	1	0.94	0.51	Tillack et al. [173]	3	0.62–0.93	0.01–1.07	Dong et al. [174]
	Total	2	0.74–0.94	0.51–0.57	1	3	0.62–0.93	0.01–1.07	
	ALI	1	0.3	0.72	Pu et al. [142]	1	0.94	0.44	Liang et al. [175]
10.0–39.9 m	ASTER	1		1.94	Menzies et al. [176]	2	0.85	0.4–1.94	Han and Qu [177]
	CHRIS	2	0.78–0.92	0.49–0.53	Wang et al. [178]	1	0.91	0.55	Lin et al. [86]
	DEIMOS-1	0				1	0.58	1	Vuolo et al. [179]
	EO-1 Hyperion	6	0.3–0.71	0.52–0.7	Varvia et al. [96]	3	0.51–0.70	0.55	Wu et al. [180]
	GF-1	0				1	0.87	0.14	He et al. [181]
	HJ-1	0				4	0.76–0.89	0.13–0.61	He et al. [181]
	IRS P6 LISS 3	2	0.63–0.85	0.61	Zhang et al. [83]	1	0.45–0.66		Rao et al. [182]
	Landsat	22	0.24–0.96	0.14–0.93	Blinn et al. [183]	17	0.66–0.98	0.13–0.93	Su et al. [92]
	Sentinel	2	0.45–0.79	0.70–0.88	Meyer et al. [81]	9	0.54–0.95	0.36–0.84	Pasqualotto et al. [184]
	SPOT	9	0.2–0.94	0.45–1.2	Gu et al. [185]	2	0.88–0.94	0.14–0.78	Houborg et al. [186]
	Total	45	0.2–0.96	0.14–1.94		42	0.45–0.98	0.14–1.94	
250 m–1.5 km	AVHRR	1	0.46	N/A	Wang et al. [187]	0			
	MERIS	1	0.64	1.15	Bacour et al. [126]	1	0.64	1.15	Bacour et al. [126]
	MISR	2	0.42–0.83	0.30–0.93	Liu et al. [94]	2	0.42–0.83	0.3–0.93	Liu et al. [94]
	MODIS	21	0.14–0.91	0.2–2.41	Alexandridis et al. [188]	14	0.60–0.93	0.01–0.64	Qiao et al. [82]
	SPOT VEGETATION	3	0.46–0.85	1.1–1.3	Baret et al. [137]	2	0.85	1.1–1.3	Baret et al. [137]
	Total	28	0.14–0.91	0.2–1.15		19	0.68–0.93	0.01–1.3	
Grand Total		84	0.14–0.96	0.14–1.94		66	0.45–0.98	0.01–1.94	

6. Challenges and Future Research

Accurately estimating LAI can improve forest and agricultural management and health monitoring. Increasing access to remote sensing technology facilitates large area estimation and provides an objective means to evaluate resources. This section presents limitations and future research directions for forest and crop LAI estimation from four aspects: data source, estimation models, scale effects, and uncertainty issues.

6.1. Data Source

Agricultural systems often have singular vegetation type, greater homogeneity, and are frequently more easily accessible than forest systems. Therefore, this tends to make application of a wide range of remote sensing data appropriate for agricultural systems. Another advantage of the often-smaller agricultural management areas is that this can make it easier for crop managers to obtain high quality time-series information, for example using unmanned airborne optical systems. Conversely, the complex structure and frequent mixing of species found in forest systems can provide challenges for passive data, hence lidar data has proved to be particularly important to detect forest canopy structure and generate LAI data for forest systems. Compared to optical data sources, active data can mitigate the impact of saturation problems and radar data can provide particular advantages for crop managers to acquire LAI information when working under cloudy weather conditions [35,58,64,189–191]. The increasing availability of active remote sensing data is likely to stimulate greater application of radar and lidar data for forest and crop LAI estimation. The fusion of multiple data sources, such as data with different spatial, spectral, or temporal resolutions, and the combination of active and passive data, is also likely to be a continued research direction.

6.2. Model Comparison and Application

Empirical, physical, and hybrid models all have advantages and application limitations. Section 4.2 showed that empirical methods are flexible and effective approaches across a range of data types and applications in identifying the relationship between LAI and spectral reflectance data. However, these methods are based on a large amount of statistical data and can only be applied within a relatively localized area because their performance is highly dependent on vegetation types, canopy structures, sensors, and temporal change [70]. The model performance variations are also illustrated in Table 3. In addition, redundant independent variables can give rise to models that overfit and thus have reduced prediction ability. Another limitation of empirical methods relates to saturation problems. Although some studies indicated that modified indexes can mitigate saturation [192–195], this problem cannot be totally avoided when using optical imagery. The majority of the literature focuses on conventional statistically focused empirical models. The application of machine learning in empirical models provides avenues for estimating forest and crop LAI. However, regardless of the method applied, the need for global training dataset acquisition remains a challenge for training empirical models [112].

In contrast to empirical methods, the theoretical foundation of physical models for LAI estimation generally result in a solution developed without strong reliance on field measurements [127]. The great promise of the physically based methods is that they can be better generalized in space and time than empirical methods, which tend to be site-, time-, and sensor-specific [196] (Table 3). Several physical models were presented in Section 4.3. Table 3 shows that PROSAIL is the most popular radiative transfer model, with the next being the four-scale model [89] that has been used for generating global LAI products, e.g., GLOBCARBON [89]. A defined physical basis gives physical models stronger spatial and temporal capability, but they are complicated, have many data input requirements, and are time-consuming to utilize [70]. Another challenge in using physical models is the so called “ill-posed” problem [13,197]. The ill-posed problem comes from the large number of input parameters that are often required within the physical model [198,199]. Researchers have found that utilizing prior

knowledge is an effective way to reduce the complexity and computation time associated with the physical model, but challenges remain [200,201]. Research to better quantify the weight and clear function of each parameter could also help improve radiative transfer methods. Inversion algorithms are also an important part for LAI retrieval based on physical models. Current inversion algorithms are computationally intensive compared with empirical models [202], primarily due to the excessive model input parameterization needed to find an optimal solution.

Hybrid models combine empirical methods, including regression and various machine learning methods, and physical models. As mentioned in Section 4.4, the current trend for forest and crop LAI estimation is the exploration of new algorithms based on machine learning methods, especially for big data calculation. However, there are still challenges with the use of hybrid models; because hybrid models integrate the methods of empirical models, they tend to inherit the critical problems of instability, which is demonstrated in Table 3 in terms of model performance, and overfitting. Exploration of new inversion algorithms and future advancement of physical models that can reduce complexity and explain radiative transfer methods with simple and more explicit functions could help improve the efficiency and accuracy of LAI estimation.

Empirical, physical, and hybrid models have all been applied to forest and crop LAI estimation. Based on the range of R^2 and RMSE for different models (Table 3), when compared to forest LAI estimation, crop LAI estimation provided a small variation across different models and it is likely that uniformity of background and vegetation types of crops reduce model uncertainty. Forest and agricultural managers need to select a model that best matches the demands of their application. Empirical models are often the preferred choice because they are relatively simple to apply. The number of VIs proposed for both forest and crop LAI estimation indicates the significance of exploring simple models. However, these models are not universally applicable and need ground LAI measurements and additional time for calibration. Although there are still challenges with the use of physical models that need to be resolved, the current trend for forest and crop LAI estimation appears to be moving in this direction because physical models are based on physical mechanisms that do not depend on field measurements [202]. The advancement of the integration of machine learning-based algorithms with physical models provides a future direction for producing general models that can be trained locally to estimate forest and crop LAI.

6.3. Scale Effect

Hyperspectral remote sensing data can record detailed spectral information, hence changes in spectral scale impact optimal band selection. However, the limited access to hyperspectral data sources has hindered deep exploration of spectral scale effects. A much larger number of studies have used data from sensors with a wide range of spatial resolutions to explore the impact of spatial scale on LAI estimation. Unfortunately, while these studies led to general conclusions, such as models that use lower spatial resolution inputs tend to underestimate LAI [88,156,203], factors such as pixel heterogeneity and model robustness that also impact how effective a dataset will be for estimating forest and crop LAI are not well characterized. Chai et al. [70] and Gray and Song [69] took advantage of multiple data sources, including high spatial and high temporal resolution datasets, to reduce the scale effects observed in low spatial resolution information and improve LAI estimation. However, there is still a need to consider how to build LAI estimation models that are applicable across different spatial scales or explore how to utilize scale transformation algorithms to make different spatial scales compatible with LAI estimation models. Empirical methods, mathematical models, and fractal theory have been explored to characterize the relationship between different scales for LAI estimation, but the quantitative impact of variation of different scales of remote sensing data is still unknown.

Ground validation is also a factor in considering scale effects on LAI estimation. Baret et al. [159] and Xu et al. [160] explored ground sampling and upscaling methods to mitigate the scale effects stemming from the mismatched scale between remote sensing data sources and ground measurements. However, while these studies provide an important step forward, a fundamental issue that remains

unresolved is quantifying the relationship between scales. Future studies need to focus on this in order to make full use of remote sensing data from different sensors. Quantifying the scale relationships will facilitate greater flexibility in terms of incorporating multi-sensor data into a single model. Exploring quantitative scale effects can also help to improve the accuracy of continuous forest and crop LAI estimation and help forest and agricultural managers efficiently incorporate multiple data sources.

6.4. The Uncertainty of LAI Estimation

The uncertainty in LAI products can be categorized as theoretical or physical [204]. Theoretical uncertainty is caused by both uncertainty in the input data and from model imperfections and is usually evaluated by model builders. Sources of theoretical uncertainty include ground LAI measurements [205], remote sensing data source, data preprocessing, model parameters, model saturation, model internal mechanisms, environmental factors (e.g., weather condition), topography effects, and the range of natural variation in biophysical parameters not accounted for in the model [177,206]. By comparison, physical uncertainties are evaluated by model users through comparison with ground validation data, such as field measurements or estimations from higher-resolution imagery [207]. The physical uncertainty is often characterized by predictive performance, e.g., RMSE. Yan et al. [26] reviewed indirect ground LAI measurement methods and concluded that sampling and scale effect are critical issues in terms of indirect ground LAI measurements, yet these factors have been minimally studied and more research is needed. Yan et al. [26] also suggested that consistent methods and instruments are critical for ground LAI collection.

Building from the advantages and disadvantages of different detection systems presented previously (Table 2), Table 6 summarizes the main sources uncertainty source for different detection systems. This table highlights the increased sources of uncertainty in passive remote sensing data compared to active remote sensing data. The improvement of data preprocessing and the exploration of standard procedures for radiometric, geometric, and atmospheric correction during the last three decades has reduced uncertainty associated with the use of remote sensing data [208–210]. To explore spatial scale effects, Yao et al. [211] determined corn LAI inversion physical uncertainty within mixed pixels and concluded that the absolute error of LAI estimation could decrease by up to 0.4 as the vegetation percentage in a mixed pixel increased. While there have been studies that explored the variation of LAI estimation across different spatial resolutions, quantitative estimates of physical uncertainty and the spatial scale effect on LAI estimation has not been investigated. Furthermore, few studies have considered if there are differences in terms of scale impact for forest versus crop LAI estimation. Within a given ground sample, unit forest systems tend to have higher heterogeneity due to a more complex structure and background compared to agricultural systems, hence differences are likely.

Table 6. Uncertainty sources for different detection systems.

Passive Remote Sensing	Active Remote Sensing	
	Lidar	Radar
Data processing	×	×
Saturation	×	
Weather	×	×
Topography effects *	×	×
Spatial scale effects *	×	×

* Denotes effects that are more significant for forest than crop LAI estimation.

Estimation models impact LAI uncertainty since different models will derive different results even from the same or similar data sources. For example, most global LAI products are derived from coarse resolution data but Chen [22] indicated that there are large differences among existing global LAI products and the model applied is one of the factors that led to these differences. With respect to

physical models, which are analyzed from a radiative transfer viewpoint and tend to provide more stable results for LAI estimation than empirical models, it is critical to understand the importance of variables included and their effect on uncertainty. Wang et al. [206] proposed a stabilized uncertainty function to demonstrate that accurate specification of algorithm input uncertainty is critical for LAI estimation and that the more accurate inputs are, the more accurate the algorithm output will be.

Local topography can also have significant effects on field measurements of LAI and remote sensing-based LAI estimation models [46]. For example, derived layers such as the enhanced vegetation index (EVI) that are often used in empirical LAI estimation models are sensitive to topographic effects, yet available products, e.g., MODIS EVI, are not corrected for this factor [212]. Topographic effects are particularly problematic for forest LAI estimation over mountain areas and across different spatial scales [213]. The review by Fang et al. [46] suggests several approaches for mitigating topographic effects including performing topographic corrections of field or remote sensing data, incorporating topographic variables in models, and creating models for different classes of topographic variables.

LAI uncertainty is also dependent on the natural variation in LAI associated with growth stages and vegetation type. Green et al. [28] and Fang et al. [46] found that high precision values were found at low LAI values due to the saturation issues in estimating high LAI values. Yao et al. [214] used Bayes theorem to apply a priori knowledge in the model inversion and demonstrated that some models performed better for LAI estimation at early growth stages compared to later growth stages. Fang et al. [207] used product quantitative quality indicators to assess LAI product uncertainty and their results showed that the highest relative uncertainty usually appeared in ecological transition zones. Chen [22] identified different LAI seasonal variation patterns for conifer and deciduous forest. These studies suggest that the uncertainty of LAI estimation is impacted by vegetation type as well as time within the growing season. For example, forest LAI was underestimated by as much as 1.5 in the summer due to the seasonal decrease of the red reflectance attributed to the background (all the materials below the forest canopy). Conifer forest LAI was underestimated by nearly 100% in the winter due to the snow cover [215]. However, knowing that this is not the only source of LAI uncertainty, quantifying uncertainty for different vegetation types is challenging. As discussed earlier in the paper, uncertainty can be characterized from theoretical and physical perspectives. While physical uncertainty is likely more of interest to the user community, exploration of theoretical uncertainty can help understand sources of physical uncertainty and improve LAI estimation. Bayesian approaches could provide theoretical uncertainty measures from posterior distribution and concurrent estimation of LAI based on uncertainty of input parameters [96,177,216,217]. Han and Qu [177] and Qu et al. [217] used Bayesian approaches to conclude that the addition of high-resolution remote sensing observation data improved LAI estimation models and increase model reliability. The study performed by Varvia et al. [218] showed that Bayesian LAI estimates that account for model uncertainties outperformed conventional estimates based on VI regression methods.

The number of studies that focus on uncertainty in LAI estimation is small. There are limited studies that explore quantification of uncertainty in model inputs and other sources, including parameters mentioned at the beginning of this section. The quantitative effects on the LAI estimation from these parameters are still unresolved. However, those studies that have explored this area indicate that Bayesian approaches are a critical area for further research and have a bright future for analysis of the uncertainty of LAI estimates.

7. Conclusions and Recommendations

Improving forest and crop LAI estimation from remotely sensed data depends on greater utilization of diverse data sources, continued model enhancement, and further exploration of scale effects. There are few studies that report the use of lidar remote sensing for crop LAI estimation, while radar remote sensing has limited application for forest LAI estimation. The expanded use and fusion of different data sources and data types provides opportunities to improve LAI estimation accuracy, consistency, and efficiency.

Beyond the data applied, there are opportunities to improve LAI estimation through continued development of empirical, physical, and hybrid models. In the short-term, without general models, empirical models that require local validation are currently recommended for forest and crop managers. However, continued work is needed to focus on using new inversion algorithms based on machine learning methods to develop general models that mitigate the “ill-posed” problem associated with physical model inversion. This will require the study of physical mechanisms of radiative transfer to integrate local physiology and biochemistry parameter datasets from different sites and temperature zones.

A challenge in creating more generally applicable LAI estimation models is quantifying the scale effects arising from application of images with various resolutions that lead to variable accuracy for LAI estimation. Quantitative exploration of the scale relationship from different sensors can facilitate the utilization of multiple data sources. Spatial scale effects appear to play a more important role for forest LAI estimation as compared to agricultural applications, which is likely related to the impact of the greater pixel heterogeneity typical in forests.

More extensive use of methods to quantify uncertainty is needed to improve rigor in forest and crop LAI estimation and validation. Bayesian approaches have been demonstrated as an effective method to quantify the uncertainty of LAI estimation based on the uncertainty of the input parameters that affect LAI estimation. Further analysis is needed in order to better analyze the quantitative effects of remote sensing data source, ground measurements, and related environmental factors on LAI estimation.

The theoretical uncertainty of ground measurements, influence of scale mismatches, and the uncertainty of LAI estimation are all interrelated. It is necessary to establish an appropriate experimental design to explore scale effects, while taking into account the quantitative uncertainty of input factors in order to better understand and mitigate these challenges. Through enhancing data applications, models, and uncertainty source analysis, remote sensing-based forest and crop LAI estimation models will have greater potential to provide critical support of forest and agricultural management practices.

Supplementary Materials: The following are available online at <http://www.mdpi.com/2072-4292/12/18/2934/s1>, An expanded reference list that summarizes the different detection systems (Table S1: Detection systems used for remote sensing of leaf area index measurement in 190 papers published between 1990–2019) and LAI estimation models (Table S2: Models used for remote sensing of leaf area index measurement in 190 papers published between 1990–2019) used in the 190 published papers.

Author Contributions: Conceptualization, J.X., L.J.Q., T.A.V., and J.I.; methodology, J.X., L.J.Q., T.A.V., and J.I.; writing—original draft preparation, J.X.; writing—review and editing, J.X., L.J.Q., T.A.V., and J.I. All authors have read and agreed to the published version of the manuscript.

Funding: This work was supported by the State University of New York College of Environmental Science and Forestry (SUNY ESF), and Honeywell International. Jungho Im was partially supported by the Korea Environment Industry & Technology Institute (KEITI) through its Urban Ecological Health Promotion Technology Development Project funded by the Korea Ministry of Environment (MOE) (2020002770001).

Conflicts of Interest: The authors declare no conflict of interest.

References

1. Hansen, M.C.; Potapov, P.V.; Moore, R.; Hancher, M.; Turubanova, S.; Tyukavina, A.; Thau, D.; Stehman, S.; Goetz, S.; Loveland, T. High-resolution global maps of 21st-century forest cover change. *Science* **2013**, *342*, 850–853. [[CrossRef](#)]
2. Vanclay, J.K. *Modelling Forest Growth and Yield: Applications to Mixed Tropical Forests*; CABI: Wallingford, UK, 1994; p. 537.
3. Ryan, M.G.; Binkley, D.; Fownes, J.H.; Giardina, C.P.; Senock, R.S. An experimental test of the causes of forest growth decline with stand age. *Ecol. Monogr.* **2004**, *74*, 393–414. [[CrossRef](#)]
4. Saxe, H.; Cannell, M.G.; Johnsen, Ø.; Ryan, M.G.; Vourlitis, G. Tree and forest functioning in response to global warming. *New Phytol.* **2001**, *149*, 369–399. [[CrossRef](#)]

5. Flannigan, M.D.; Amiro, B.D.; Logan, K.A.; Stocks, B.; Wotton, B. Forest fires and climate change in the 21st century. *Mitigation Adapt. Strat. Glob. Chang.* **2006**, *11*, 847–859. [[CrossRef](#)]
6. Liu, Y.; Stanturf, J.; Goodrick, S. Trends in global wildfire potential in a changing climate. *For. Ecol. Manag.* **2010**, *259*, 685–697. [[CrossRef](#)]
7. Myneni, R.B.; Hoffman, S.; Knyazikhin, Y.; Privette, J.; Glassy, J.; Tian, Y.; Wang, Y.; Song, X.; Zhang, Y.; Smith, G. Global products of vegetation leaf area and fraction absorbed PAR from year one of MODIS data. *Remote Sens. Environ.* **2002**, *83*, 214–231. [[CrossRef](#)]
8. Zarco-Tejada, P.; Sepulcre-Cantó, G. Remote sensing of vegetation biophysical parameters for detecting stress condition and land cover changes. In Proceedings of the Jornadas de Investigación de la Zona no Saturada del Suelo, VIII, Cordoba, Spain, 14–16 November 2007; pp. 37–44.
9. Neilson, R.P.; Drapek, R.J. Potentially complex biosphere responses to transient global warming. *Glob. Chang. Biol.* **1998**, *4*, 505–521. [[CrossRef](#)]
10. Ruimy, A.; Saugier, B.; Dedieu, G. Methodology for the estimation of terrestrial net primary production from remotely sensed data. *J. Geophys. Res. Atoms.* **1994**, *99*, 5263–5283. [[CrossRef](#)]
11. Bonan, G.B. Importance of leaf area index and forest type when estimating photosynthesis in boreal forests. *Remote Sens. Environ.* **1993**, *43*, 303–314. [[CrossRef](#)]
12. Running, S.W.; Nemani, R.R.; Heinsch, F.A.; Zhao, M.; Reeves, M.; Hashimoto, H. A continuous satellite-derived measure of global terrestrial primary production. *AIBS Bull.* **2004**, *54*, 547–560. [[CrossRef](#)]
13. Wang, R.; Chen, J.M.; Liu, Z.; Arain, A. Evaluation of seasonal variations of remotely sensed leaf area index over five evergreen coniferous forests. *ISPRS J. Photogramm. Remote Sens.* **2017**, *130*, 187–201. [[CrossRef](#)]
14. Curnel, Y.; de Wit, A.J.; Duveiller, G.; Defourny, P. Potential performances of remotely sensed LAI assimilation in WOFOST model based on an OSS Experiment. *Agric. For. Meteorol.* **2011**, *151*, 1843–1855. [[CrossRef](#)]
15. Treitz, P.M.; Howarth, P.J. Hyperspectral remote sensing for estimating biophysical parameters of forest ecosystems. *Prog. Phys. Geogr.* **1999**, *23*, 359–390. [[CrossRef](#)]
16. Chen, J.M.; Cihlar, J. Retrieving leaf area index of boreal conifer forests using Landsat TM images. *Remote Sens. Environ.* **1996**, *55*, 153–162. [[CrossRef](#)]
17. Carlson, T.N.; Ripley, D.A. On the relation between NDVI, fractional vegetation cover, and leaf area index. *Remote Sens. Environ.* **1997**, *62*, 241–252. [[CrossRef](#)]
18. Wu, C.; Niu, Z.; Wang, J.; Gao, S.; Huang, W. Predicting leaf area index in wheat using angular vegetation indices derived from in situ canopy measurements. *Can. J. Remote Sens.* **2010**, *36*, 301–312. [[CrossRef](#)]
19. Breda, N.J. Ground-based measurements of leaf area index: A review of methods, instruments and current controversies. *J. Exp. Bot.* **2003**, *54*, 2403–2417. [[CrossRef](#)]
20. Jonckheere, I.; Fleck, S.; Nackaerts, K.; Muys, B.; Coppin, P.; Weiss, M.; Baret, F. Review of methods for in situ leaf area index determination: Part I. Theories, sensors and hemispherical photography. *Agric. For. Meteorol.* **2004**, *121*, 19–35. [[CrossRef](#)]
21. Weiss, M.; Baret, F.; Smith, G.; Jonckheere, I.; Coppin, P. Review of methods for in situ leaf area index (LAI) determination: Part II. Estimation of LAI, errors and sampling. *Agric. For. Meteorol.* **2004**, *121*, 37–53. [[CrossRef](#)]
22. Chen, J.M. Remote sensing of leaf area index of vegetation covers. In *Remote Sensing of Natural Resources*; CRC Press: Boca Raton, FL, USA, 2013; pp. 375–398. [[CrossRef](#)]
23. Qu, Y. Leaf Area Index: Advance on the Ground-Based Measurement. In *Observation and Measurement of Ecohydrological Processes*; Li, X., Vereecken, H., Eds.; Springer: Berlin/Heidelberg, Germany, 2018; pp. 1–20. [[CrossRef](#)]
24. Gower, S.T.; Kucharik, C.J.; Norman, J.M. Direct and Indirect Estimation of Leaf Area Index, fAPAR, and Net Primary Production of Terrestrial Ecosystems. *Remote Sens. Environ.* **1999**, *70*, 29–51. [[CrossRef](#)]
25. Chen, J.M.; Rich, P.M.; Gower, S.T.; Norman, J.M.; Plummer, S. Leaf area index of boreal forests: Theory, techniques, and measurements. *J. Geophys. Res. Atmos.* **1997**, *102*, 29429–29443. [[CrossRef](#)]
26. Yan, G.; Hu, R.; Luo, J.; Weiss, M.; Jiang, H.; Mu, X.; Xie, D.; Zhang, W. Review of indirect optical measurements of leaf area index: Recent advances, challenges, and perspectives. *Agric. For. Meteorol.* **2019**, *265*, 390–411. [[CrossRef](#)]
27. Zheng, G.; Moskal, L.M. Retrieving leaf area index (LAI) using remote sensing: Theories, methods and sensors. *Sensors* **2009**, *9*, 2719–2745. [[CrossRef](#)] [[PubMed](#)]

28. Green, E.P.; Mumby, P.J.; Edwards, A.J.; Clark, C.D.; Ellis, A.C. Estimating leaf area index of mangroves from satellite data. *Aquat. Bot.* **1997**, *58*, 11–19. [[CrossRef](#)]
29. Wulder, M.A. Optical remote-sensing techniques for the assessment of forest inventory and biophysical parameters. *Prog. Phys. Geogr.* **1998**, *22*, 449–476. [[CrossRef](#)]
30. Weng, Q. *Scale Issues in Remote Sensing*; John Wiley & Sons: Hoboken, NJ, USA, 2014. [[CrossRef](#)]
31. Wu, H.; Li, Z. Scale issues in remote sensing: A review on analysis, processing and modeling. *Sensors* **2009**, *9*, 1768–1793. [[CrossRef](#)]
32. Baret, F.; Buis, S. Estimating canopy characteristics from remote sensing observations: Review of methods and associated problems. In *Advances in Land Remote Sensing*; Springer: Dordrecht, The Netherlands, 2008; pp. 173–201. [[CrossRef](#)]
33. Song, C. Optical remote sensing of forest leaf area index and biomass. *Prog. Phys. Geogr.* **2013**, *37*, 98–113. [[CrossRef](#)]
34. Richardson, J.J.; Moskal, L.M.; Kim, S.-H. Modeling approaches to estimate effective leaf area index from aerial discrete-return LIDAR. *Agric. For. Meteorol.* **2009**, *149*, 1152–1160. [[CrossRef](#)]
35. Arnó, J.; Vallès, J.M.; Llorens, J.; Sanz, R.; Masip, J.; Palacín, J.; Rosell-Polo, J.R. Leaf area index estimation in vineyards using a ground-based LiDAR scanner. *Precis. Agric.* **2012**, *14*, 290–306. [[CrossRef](#)]
36. McNairn, H.; Brisco, B. The application of C-band polarimetric SAR for agriculture: A review. *Can. J. Remote Sens.* **2004**, *30*, 525–542. [[CrossRef](#)]
37. Pix4D. *Pix4Dmapper 4.1 User Manual*; Pix4D SA: Lausanne, Switzerland, 2017.
38. Zhang, C.; Kovacs, J.M. The application of small unmanned aerial systems for Precis. Agric.: A review. *Precis. Agric.* **2012**, *13*, 693–712. [[CrossRef](#)]
39. Roosjen, P.P.; Brede, B.; Suomalainen, J.M.; Bartholomeus, H.M.; Kooistra, L.; Clevers, J.G. Improved estimation of leaf area index and leaf chlorophyll content of a potato crop using multi-angle spectral data—potential of unmanned aerial vehicle imagery. *Int. J. Appl. Earth Obs. Geoinf.* **2018**, *66*, 14–26. [[CrossRef](#)]
40. Tian, J.; Wang, L.; Li, X.; Gong, H.; Shi, C.; Zhong, R.; Liu, X. Comparison of UAV and WorldView-2 imagery for mapping leaf area index of mangrove forest. *Int. J. Appl. Earth Obs. Geoinf.* **2017**, *61*, 22–31. [[CrossRef](#)]
41. Spanner, M.A.; Pierce, L.L.; Peterson, D.L.; Running, S.W. Remote sensing of temperate coniferous forest leaf area index The influence of canopy closure, understory vegetation and background reflectance. *Int. J. Remote Sens.* **1990**, *11*, 95–111. [[CrossRef](#)]
42. Dash, J.; Ongutu, B.O. Recent advances in space-borne optical remote sensing systems for monitoring global terrestrial ecosystems. *Prog. Phys. Geogr. Earth Environ.* **2016**, *40*, 322–351. [[CrossRef](#)]
43. Roy, D.P.; Wulder, M.A.; Loveland, T.R.; Woodcock, C.E.; Allen, R.G.; Anderson, M.C.; Helder, D.; Irons, J.R.; Johnson, D.M.; Kennedy, R.; et al. Landsat-8: Science and product vision for terrestrial global change research. *Remote Sens. Environ.* **2014**, *145*, 154–172. [[CrossRef](#)]
44. Drusch, M.; Del Bello, U.; Carlier, S.; Colin, O.; Fernandez, V.; Gascon, F.; Hoersch, B.; Isola, C.; Laberinti, P.; Martimort, P.; et al. Sentinel-2: ESA's Optical High-Resolution Mission for GMES Operational Services. *Remote Sens. Environ.* **2012**, *120*, 25–36. [[CrossRef](#)]
45. Campos-Taberner, M.; García-Haro, F.; Busetto, L.; Ranghetti, L.; Martínez, B.; Gilabert, M.A.; Camps-Valls, G.; Camacho, F.; Boschetti, M. A critical comparison of remote sensing leaf area index estimates over rice-cultivated areas: From Sentinel-2 and Landsat-7/8 to MODIS, GEOP1 and EUMETSAT polar system. *Remote Sens.* **2018**, *10*, 763. [[CrossRef](#)]
46. Fang, H.; Baret, F.; Plummer, S.; Schaepman-Strub, G. An overview of global leaf area index (LAI): Methods, products, validation, and applications. *Rev. Geophys.* **2019**. [[CrossRef](#)]
47. Lim, K.; Treitz, P.; Wulder, M.; St-Onge, B.; Flood, M. LiDAR remote sensing of forest structure. *Prog. Phys. Geogr.* **2003**, *27*, 88–106. [[CrossRef](#)]
48. Vincent, R. RADAR|Synthetic Aperture Radar (Land Surface Applications). In *Encyclopedia of Atmospheric Sciences*; Elsevier Ltd.: Amsterdam, The Netherlands, 2015; Volume 4, pp. 470–476.
49. Aggarwal, S. Principles of remote sensing. In Proceedings of the Satellite Remote Sensing and GIS Applications in Agricultural Meteorology Training Workshop, Dehra Dun, India, 7–11 July 2003; pp. 23–38.
50. Walther, T.; Fry, E.S. Optics in Remote Sensing. In *Optics in Our Time*; Al-Amri, M.D., El-Gomati, M., Zubairy, M.S., Eds.; Springer International Publishing: Cham, Switzerland, 2016; pp. 201–222. [[CrossRef](#)]

51. Ilangakoon, N.T.; Gorsevski, P.V.; Simic Milas, A. Estimating leaf area index by bayesian linear regression using terrestrial Lidar, LAI-2200 plant canopy analyzer, and landsat tm spectral indices. *Can. J. Remote Sens.* **2015**, *41*, 315–333. [[CrossRef](#)]
52. Moorthy, I.; Miller, J.R.; Hu, B.; Chen, J.; Li, Q. Retrieving crown leaf area index from an individual tree using ground-based lidar data. *Can. J. Remote Sens.* **2008**, *34*, 320–332. [[CrossRef](#)]
53. Strahler, A.H.; Jupp, D.L.; Woodcock, C.E.; Schaaf, C.B.; Yao, T.; Zhao, F.; Yang, X.; Lovell, J.; Culvenor, D.; Newnham, G. Retrieval of forest structural parameters using a ground-based lidar instrument (Echidna[®]). *Can. J. Remote Sens.* **2008**, *34*, S426–S440. [[CrossRef](#)]
54. Jupp, D.L.; Culvenor, D.; Lovell, J.; Newnham, G.; Strahler, A.; Woodcock, C. Estimating forest LAI profiles and structural parameters using a ground-based laser called Echidna[®]. *Tree Physiol.* **2009**, *29*, 171–181. [[CrossRef](#)] [[PubMed](#)]
55. Zhao, K.; García, M.; Liu, S.; Guo, Q.; Chen, G.; Zhang, X.; Zhou, Y.; Meng, X. Terrestrial lidar remote sensing of forests: Maximum likelihood estimates of canopy profile, leaf area index, and leaf angle distribution. *Agric. For. Meteorol.* **2015**, *209*, 100–113. [[CrossRef](#)]
56. Lovell, J.; Jupp, D.L.; Culvenor, D.; Coops, N. Using airborne and ground-based ranging lidar to measure canopy structure in Australian forests. *Can. J. Remote Sens.* **2003**, *29*, 607–622. [[CrossRef](#)]
57. Morsdorf, F.; Kötz, B.; Meier, E.; Itten, K.; Allgöwer, B. Estimation of LAI and fractional cover from small footprint airborne laser scanning data based on gap fraction. *Remote Sens. Environ.* **2006**, *104*, 50–61. [[CrossRef](#)]
58. Peduzzi, A.; Wynne, R.H.; Fox, T.R.; Nelson, R.F.; Thomas, V.A. Estimating leaf area index in intensively managed pine plantations using airborne laser scanner data. *For. Ecol. Manag.* **2012**, *270*, 54–65. [[CrossRef](#)]
59. Lin, Y.; West, G. Retrieval of effective leaf area index (LAIE) and leaf area density (LAD) profile at individual tree level using high density multi-return airborne LiDAR. *Int. J. Appl. Earth Obs. Geoinf.* **2016**, *50*, 150–158. [[CrossRef](#)]
60. Luo, S.; Chen, J.M.; Wang, C.; Gonsamo, A.; Xi, X.; Lin, Y.; Qian, M.; Peng, D.; Nie, S.; Qin, H. Comparative performances of airborne LiDAR height and intensity data for leaf area index estimation. *IEEE J. Sel. Top. Appl. Earth Obs. Remote Sens.* **2018**, *11*, 300–310. [[CrossRef](#)]
61. Cui, Y.; Zhao, K.; Fan, W.; Xu, X. Retrieving crop fractional cover and LAI based on airborne Lidar data. *J. Remote Sens.* **2011**, *15*, 1276–1288. [[CrossRef](#)]
62. Nie, S.; Wang, C.; Dong, P.; Xi, X. Estimating leaf area index of maize using airborne full-waveform lidar data. *Remote Sens. Lett.* **2016**, *7*, 111–120. [[CrossRef](#)]
63. Sadro, S.; Gastil-Buhl, M.; Melack, J. Characterizing patterns of plant distribution in a southern California salt marsh using remotely sensed topographic and hyperspectral data and local tidal fluctuations. *Remote Sens. Environ.* **2007**, *110*, 226–239. [[CrossRef](#)]
64. Hosseini, M.; McNairn, H.; Merzouki, A.; Pacheco, A. Estimation of Leaf Area Index (LAI) in corn and soybeans using multi-polarization C-and L-band radar data. *Remote Sens. Environ.* **2015**, *170*, 77–89. [[CrossRef](#)]
65. Paloscia, S. An empirical approach to estimating leaf area index from multifrequency SAR data. *Int. J. Remote Sens.* **1998**, *19*, 359–364. [[CrossRef](#)]
66. Afzal, R.S.; Anthony, W.Y.; Dallas, J.L.; Melak, A.; Lukemire, A.T.; Ramos-Izqueirido, L.; Mamakos, W. The geoscience laser altimeter system (GLAS) laser transmitter. *IEEE J. Sel. Top. Quantum Electron.* **2007**, *13*, 511–536. [[CrossRef](#)]
67. Tang, H.; Brolly, M.; Zhao, F.; Strahler, A.H.; Schaaf, C.L.; Ganguly, S.; Zhang, G.; Dubayah, R. Deriving and validating Leaf Area Index (LAI) at multiple spatial scales through lidar remote sensing: A case study in Sierra National Forest, CA. *Remote Sens. Environ.* **2014**, *143*, 131–141. [[CrossRef](#)]
68. Inoue, Y.; Sakaiya, E.; Wang, C. Capability of C-band backscattering coefficients from high-resolution satellite SAR sensors to assess biophysical variables in paddy rice. *Remote Sens. Environ.* **2014**, *140*, 257–266. [[CrossRef](#)]
69. Gray, J.; Song, C. Mapping leaf area index using spatial, spectral, and temporal information from multiple sensors. *Remote Sens. Environ.* **2012**, *119*, 173–183. [[CrossRef](#)]
70. Chai, L.; Qu, Y.; Zhang, L.; Liang, S.; Wang, J. Estimating time-series leaf area index based on recurrent nonlinear autoregressive neural networks with exogenous inputs. *Int. J. Remote Sens.* **2012**, *33*, 5712–5731. [[CrossRef](#)]

71. Koetz, B.; Sun, G.; Morsdorf, F.; Ranson, K.; Kneubühler, M.; Itten, K.; Allgöwer, B. Fusion of imaging spectrometer and LIDAR data over combined radiative transfer models for forest canopy characterization. *Remote Sens. Environ.* **2007**, *106*, 449–459. [[CrossRef](#)]
72. Gao, S.; Niu, Z.; Huang, N.; Hou, X. Estimating the Leaf Area Index, height and biomass of maize using HJ-1 and RADARSAT-2. *Int. J. Appl. Earth Obs. Geoinf.* **2013**, *24*, 1–8. [[CrossRef](#)]
73. Yang, X.; Wang, C.; Pan, F.; Nie, S.; Xi, X.; Luo, S. Retrieving leaf area index in discontinuous forest using ICESat/GLAS full-waveform data based on gap fraction model. *ISPRS J. Photogramm. Remote Sens.* **2019**, *148*, 54–62. [[CrossRef](#)]
74. Campos-Taberner, M.; García-Haro, F.J.; Camps-Valls, G.; Grau Muedra, G.; Nutini, F.; Crema, A.; Boschetti, M. Multitemporal and multiresolution leaf area index retrieval for operational local rice crop monitoring. *Remote Sens. Environ.* **2016**, *187*, 102–118. [[CrossRef](#)]
75. Tucker, C.J. Red and photographic infrared linear combinations for monitoring vegetation. *Remote Sens. Environ.* **1979**, *8*, 127–150. [[CrossRef](#)]
76. Jacquemoud, S.; Baret, F. PROSPECT: A model of leaf optical properties spectra. *Remote Sens. Environ.* **1990**, *34*, 75–91. [[CrossRef](#)]
77. Qu, Y.; Shaker, A.; Silva, C.A.; Klauberg, C.; Pinagé, E.R. Remote Sensing of Leaf Area Index from LiDAR Height Percentile Metrics and Comparison with MODIS Product in a Selectively Logged Tropical Forest Area in Eastern Amazonia. *Remote Sens.* **2018**, *10*, 970. [[CrossRef](#)]
78. Zhou, J.; Zhang, S.; Yang, H.; Xiao, Z.; Gao, F. The retrieval of 30-m resolution LAI from landsat data by combining MODIS products. *Remote Sens.* **2018**, *10*, 1187. [[CrossRef](#)]
79. Korhonen, L.; Packalen, P.; Rautiainen, M. Comparison of Sentinel-2 and Landsat 8 in the estimation of boreal forest canopy cover and leaf area index. *Remote Sens. Environ.* **2017**, *195*, 259–274. [[CrossRef](#)]
80. Li, S.; Yuan, F.; Ata-Ul-Karim, S.T.; Zheng, H.; Cheng, T.; Liu, X.; Tian, Y.; Zhu, Y.; Cao, W.; Cao, Q. Combining Color Indices and Textures of UAV-Based Digital Imagery for Rice LAI Estimation. *Remote Sens.* **2019**, *11*, 1763. [[CrossRef](#)]
81. Meyer, L.H.; Heurich, M.; Beudert, B.; Premier, J.; Pflugmacher, D. Comparison of Landsat-8 and Sentinel-2 data for estimation of leaf area index in temperate forests. *Remote Sens.* **2019**, *11*, 1160. [[CrossRef](#)]
82. Qiao, K.; Zhu, W.; Xie, Z.; Li, P. Estimating the seasonal dynamics of the leaf area index using piecewise LAI-VI relationships based on phenophases. *Remote Sens.* **2019**, *11*, 689. [[CrossRef](#)]
83. Zhang, Z.; He, G.; Wang, X.; Jiang, H. Leaf area index estimation of bamboo forest in Fujian province based on IRS P6 LISS 3 imagery. *Int. J. Remote Sens.* **2011**, *32*, 5365–5379. [[CrossRef](#)]
84. Li, W.; Niu, Z.; Chen, H.; Li, D. Characterizing canopy structural complexity for the estimation of maize LAI based on ALS data and UAV stereo images. *Int. J. Remote Sens.* **2017**, *38*, 2106–2116. [[CrossRef](#)]
85. Neinavaz, E.; Darvishzadeh, R.; Skidmore, A.K.; Abdullah, H. Integration of Landsat-8 thermal and visible-short wave infrared data for improving prediction accuracy of forest leaf area index. *Remote Sens.* **2019**, *11*, 390. [[CrossRef](#)]
86. Lin, J.; Pan, Y.; Lyu, H.; Zhu, X.; Li, X.; Dong, B.; Li, H. Developing a two-step algorithm to estimate the leaf area index of forests with complex structures based on CHRIS/PROBA data. *For. Ecol. Manag.* **2019**, *441*, 57–70. [[CrossRef](#)]
87. Banskota, A.; Serbin, S.P.; Wynne, R.H.; Thomas, V.A.; Falkowski, M.J.; Kayastha, N.; Gastellu-Etchegorry, J.-P.; Townsend, P.A. An LUT-based inversion of DART model to estimate forest LAI from hyperspectral data. *IEEE J. Sel. Top. Appl. Earth Obs. Remote Sens.* **2015**, *8*, 3147–3160. [[CrossRef](#)]
88. Liu, Y.; Ju, W.; Chen, J.; Zhu, G.; Xing, B.; Zhu, J.; He, M. Spatial and temporal variations of forest LAI in China during 2000–2010. *Chin. Sci. Bull.* **2012**, *57*, 2846–2856. [[CrossRef](#)]
89. Deng, F.; Chen, J.M.; Plummer, S.; Chen, M.; Pisek, J. Algorithm for global leaf area index retrieval using satellite imagery. *IEEE Trans. Geosci. Remote Sens.* **2006**, *44*, 2219–2229. [[CrossRef](#)]
90. Banskota, A.; Wynne, R.H.; Thomas, V.A.; Serbin, S.P.; Kayastha, N.; Gastellu-Etchegorry, J.P.; Townsend, P.A. Investigating the utility of wavelet transforms for inverting a 3-D radiative transfer model using hyperspectral data to retrieve forest LAI. *Remote Sens.* **2013**, *5*, 2639–2659. [[CrossRef](#)]
91. Le Maire, G.; Marsden, C.; Verhoef, W.; Ponzoni, F.J.; Seen, D.L.; Bégué, A.; Stape, J.-L.; Nouvellon, Y. Leaf area index estimation with MODIS reflectance time series and model inversion during full rotations of Eucalyptus plantations. *Remote Sens. Environ.* **2011**, *115*, 586–599. [[CrossRef](#)]

92. Su, W.; Huang, J.; Liu, D.; Zhang, M. Retrieving corn canopy leaf area index from multitemporal landsat imagery and terrestrial LiDAR data. *Remote Sens.* **2019**, *11*, 572. [[CrossRef](#)]
93. Ma, H.; Song, J.; Wang, J.; Xiao, Z.; Fu, Z. Improvement of spatially continuous forest LAI retrieval by integration of discrete airborne LiDAR and remote sensing multi-angle optical data. *Agric. For. Meteorol.* **2014**, *189*, 60–70. [[CrossRef](#)]
94. Liu, Q.; Liang, S.; Xiao, Z.; Fang, H. Retrieval of leaf area index using temporal, spectral, and angular information from multiple satellite data. *Remote Sens. Environ.* **2014**, *145*, 25–37. [[CrossRef](#)]
95. Gonsamo, A.; Chen, J.M. Improved LAI algorithm implementation to MODIS data by incorporating background, topography, and foliage clumping information. *IEEE Trans. Geosci. Remote Sens.* **2014**, *52*, 1076–1088. [[CrossRef](#)]
96. Varvia, P.; Rautiainen, M.; Seppänen, A. Bayesian estimation of seasonal course of canopy leaf area index from hyperspectral satellite data. *J. Quant. Spectrosc. Radiat. Transf.* **2018**, *208*, 19–28. [[CrossRef](#)]
97. Xing, L.; Li, X.; Du, H.; Zhou, G.; Mao, F.; Liu, T.; Zheng, J.; Dong, L.; Zhang, M.; Han, N. Assimilating multiresolution leaf area index of moso bamboo forest from MODIS time series data based on a Hierarchical Bayesian Network algorithm. *Remote Sens.* **2019**, *11*, 56. [[CrossRef](#)]
98. Xu, X.; Lu, J.; Zhang, N.; Yang, T.; He, J.; Yao, X.; Cheng, T.; Zhu, Y.; Cao, W.; Tian, Y. Inversion of rice canopy chlorophyll content and leaf area index based on coupling of radiative transfer and Bayesian network models. *ISPRS J. Photogramm. Remote Sens.* **2019**, *150*, 185–196. [[CrossRef](#)]
99. Shi, Y.; Wang, J.; Wang, J.; Qu, Y. A prior knowledge-based method to derive high-resolution leaf area index maps with limited field measurements. *Remote Sens.* **2017**, *9*, 13. [[CrossRef](#)]
100. Qu, Y.; Zhang, Y.; Xue, H. Retrieval of 30-m-Resolution Leaf Area Index From China HJ-1 CCD Data and MODIS Products Through a Dynamic Bayesian Network. *IEEE J. Sel. Top. Appl. Earth Obs. Remote Sens.* **2014**, *7*, 222–228. [[CrossRef](#)]
101. Wang, T.; Kang, F.; Han, H.; Cheng, X.; Zhu, J.; Zhou, W. Estimation of leaf area index from high resolution ZY-3 satellite imagery in a catchment dominated by *Larix principis-rupprechtii*, northern China. *J. For. Res.* **2019**, *30*, 603–615. [[CrossRef](#)]
102. Liu, S.; Baret, F.; Abichou, M.; Boudon, F.; Thomas, S.; Zhao, K.; Fournier, C.; Andrieu, B.; Irfan, K.; Hemmerlé, M. Estimating wheat green area index from ground-based LiDAR measurement using a 3D canopy structure model. *Agric. For. Meteorol.* **2017**, *247*, 12–20. [[CrossRef](#)]
103. Jensen, R.; Binford, M. Measurement and comparison of Leaf Area Index estimators derived from satellite remote sensing techniques. *Int. J. Remote Sens.* **2004**, *25*, 4251–4265. [[CrossRef](#)]
104. Omer, G.; Mutanga, O.; Abdel-Rahman, E.M.; Adam, E. Empirical prediction of Leaf Area Index (LAI) of endangered tree species in intact and fragmented indigenous forests ecosystems using WorldView-2 data and two robust machine learning algorithms. *Remote Sens.* **2016**, *8*, 324. [[CrossRef](#)]
105. Kanning, M.; Kühling, I.; Trautz, D.; Jarmer, T. High-resolution UAV-based hyperspectral imagery for LAI and chlorophyll estimations from wheat for yield prediction. *Remote Sens.* **2018**, *10*, 2000. [[CrossRef](#)]
106. Manninen, T.; Stenberg, P.; Rautiainen, M.; Voipio, P. Leaf area index estimation of boreal and subarctic forests Using VV/HH ENVISAT/ASAR data of various swaths. *IEEE Trans. Geosci. Remote Sens.* **2013**, *51*, 3899–3909. [[CrossRef](#)]
107. Kross, A.; McNairn, H.; Lapen, D.; Sunohara, M.; Champagne, C. Assessment of RapidEye vegetation indices for estimation of leaf area index and biomass in corn and soybean crops. *Int. J. Appl. Earth Obs. Geoinf.* **2015**, *34*, 235–248. [[CrossRef](#)]
108. Zhang, D.; Liu, J.; Ni, W.; Sun, G.; Zhang, Z.; Liu, Q.; Wang, Q. Estimation of Forest Leaf Area Index Using Height and Canopy Cover Information Extracted from Unmanned Aerial Vehicle Stereo Imagery. *IEEE J. Sel. Top. Appl. Earth Obs. Remote Sens.* **2019**, *12*, 471–481. [[CrossRef](#)]
109. Solberg, S.; Brunner, A.; Hanssen, K.H.; Lange, H.; Næsset, E.; Rautiainen, M.; Stenberg, P. Mapping LAI in a Norway spruce forest using airborne laser scanning. *Remote Sens. Environ.* **2009**, *113*, 2317–2327. [[CrossRef](#)]
110. Wulder, M.; Franklin, S.; Lavigne, M. High spatial resolution optical image texture for improved estimation of forest stand leaf area index. *Can. J. Remote Sens.* **1996**, *22*, 441–449. [[CrossRef](#)]
111. Wulder, M.A.; LeDrew, E.F.; Franklin, S.E.; Lavigne, M.B. Aerial image texture information in the estimation of northern deciduous and mixed wood forest leaf area index (LAI). *Remote Sens. Environ.* **1998**, *64*, 64–76. [[CrossRef](#)]

112. Verrelst, J.; Muñoz, J.; Alonso, L.; Delegido, J.; Rivera, J.P.; Camps-Valls, G.; Moreno, J. Machine learning regression algorithms for biophysical parameter retrieval: Opportunities for Sentinel-2 and-3. *Remote Sens. Environ.* **2012**, *118*, 127–139. [[CrossRef](#)]
113. Wang, J.; Wang, J.; Shi, Y.; Zhou, H.; Liao, L. A recursive update model for estimating high-resolution LAI based on the NARX neural network and MODIS times series. *Remote Sens.* **2019**, *11*, 219. [[CrossRef](#)]
114. Jacquemoud, S.; Verhoef, W.; Baret, F.; Bacour, C.; Zarco-Tejada, P.J.; Asner, G.P.; François, C.; Ustin, S.L. PROSPECT + SAIL models: A review of use for vegetation characterization. *Remote Sens. Environ.* **2009**, *113*, S56–S66. [[CrossRef](#)]
115. Li, X.; Strahler, A.H. Geometric-optical bidirectional reflectance modeling of the discrete crown vegetation canopy: Effect of crown shape and mutual shadowing. *IEEE Trans. Geosci. Remote Sens.* **1992**, *30*, 276–292. [[CrossRef](#)]
116. Johnson, R.; Peddle, D.; Hall, R. A modeled-based sub-pixel scale mountain terrain normalization algorithm for improved LAI estimation from airborne CASI imagery. In Proceedings of the 22nd Canadian Symposium on Remote Sensing, Victoria, BC, Canada, 21–25 August 2000; pp. 415–424.
117. Kuusk, A.; Nilson, T. A directional multispectral forest reflectance model. *Remote Sens. Environ.* **2000**, *72*, 244–252. [[CrossRef](#)]
118. Rautiainen, M.; Stenberg, P.; Nilson, T.; Kuusk, A.; Smolander, H. Application of a forest reflectance model in estimating leaf area index of Scots pine stands using Landsat-7 ETM reflectance data. *Can. J. Remote Sens.* **2003**, *29*, 314–323. [[CrossRef](#)]
119. Ni-Meister, W.; Jupp, D.L.; Dubayah, R. Modeling lidar waveforms in heterogeneous and discrete canopies. *IEEE Trans. Geosci. Remote Sens.* **2001**, *39*, 1943–1958. [[CrossRef](#)]
120. Tang, H.; Dubayah, R.; Brolly, M.; Ganguly, S.; Zhang, G. Large-scale retrieval of leaf area index and vertical foliage profile from the spaceborne waveform lidar (GLAS/ICESat). *Remote Sens. Environ.* **2014**, *154*, 8–18. [[CrossRef](#)]
121. Kuusk, A. A two-layer canopy reflectance model. *J. Quant. Spectrosc. Radiat. Transf.* **2001**, *71*, 1–9. [[CrossRef](#)]
122. Gastellu-Etchegorry, J.-P.; Demarez, V.; Pinel, V.; Zagolski, F. Modeling radiative transfer in heterogeneous 3-D vegetation canopies. *Remote Sens. Environ.* **1996**, *58*, 131–156. [[CrossRef](#)]
123. Chen, J.M.; Leblanc, S.G. A four-scale bidirectional reflectance model based on canopy architecture. *IEEE Trans. Geosci. Remote Sens.* **1997**, *35*, 1316–1337. [[CrossRef](#)]
124. Rautiainen, M.; Stenberg, P. Application of photon recollision probability in coniferous canopy reflectance simulations. *Remote Sens. Environ.* **2005**, *96*, 98–107. [[CrossRef](#)]
125. Verhoef, W. Light scattering by leaf layers with application to canopy reflectance modeling: The SAIL model. *Remote Sens. Environ.* **1984**, *16*, 125–141. [[CrossRef](#)]
126. Bacour, C.; Baret, F.; Béal, D.; Weiss, M.; Pavageau, K. Neural network estimation of LAI, fAPAR, fCover and LAIx Cab, from top of canopy MERIS reflectance data: Principles and validation. *Remote Sens. Environ.* **2006**, *105*, 313–325. [[CrossRef](#)]
127. Mananze, S.; Pôças, I.; Cunha, M. Retrieval of Maize Leaf Area Index Using Hyperspectral and Multispectral Data. *Remote Sens.* **2018**, *10*, 1942. [[CrossRef](#)]
128. Verrelst, J.; Camps-Valls, G.; Muñoz-Marí, J.; Rivera, J.P.; Veroustraete, F.; Clevers, J.G.; Moreno, J. Optical remote sensing and the retrieval of terrestrial vegetation bio-geophysical properties—A review. *ISPRS J. Photogramm. Remote Sens.* **2015**, *108*, 273–290. [[CrossRef](#)]
129. Duan, S.-B.; Li, Z.-L.; Wu, H.; Tang, B.-H.; Ma, L.; Zhao, E.; Li, C. Inversion of the PROSAIL model to estimate leaf area index of maize, potato, and sunflower fields from unmanned aerial vehicle hyperspectral data. *Int. J. Appl. Earth Obs. Geoinf.* **2014**, *26*, 12–20. [[CrossRef](#)]
130. Liang, S. Recent developments in estimating land surface biogeophysical variables from optical remote sensing. *Prog. Phys. Geogr.* **2007**, *31*, 501–516. [[CrossRef](#)]
131. Chaurasia, S.; Dadhwal, V. Comparison of principal component inversion with VI-empirical approach for LAI estimation using simulated reflectance data. *Int. J. Remote Sens.* **2004**, *25*, 2881–2887. [[CrossRef](#)]
132. Qu, Y.; Zhang, Y.; Wang, J. A dynamic Bayesian network data fusion algorithm for estimating leaf area index using time-series data from in situ measurement to remote sensing observations. *Int. J. Remote Sens.* **2012**, *33*, 1106–1125. [[CrossRef](#)]

133. Pan, J.; Yang, H.; He, W.; Xu, P. Retrieve Leaf Area Index from HJ-CCD Image Based on Support Vector Regression and Physical Model. In Proceedings of the SPIE Remote Sensing for Agriculture, Ecosystems, and Hydrology XV, Dresden, Germany, 24–26 September 2013; p. 68. [[CrossRef](#)]
134. Liang, L.; Di, L.; Zhang, L.; Deng, M.; Qin, Z.; Zhao, S.; Lin, H. Estimation of crop LAI using hyperspectral vegetation indices and a hybrid inversion method. *Remote Sens. Environ.* **2015**, *165*, 123–134. [[CrossRef](#)]
135. Danson, F.; Rowland, C.; Baret, F. Training a neural network with a canopy reflectance model to estimate crop leaf area index. *Int. J. Remote Sens.* **2003**, *24*, 4891–4905. [[CrossRef](#)]
136. Haykin, S. *Neural Networks: A Comprehensive Foundation*; Prentice Hall PTR: Upper Saddle River, NJ, USA, 1994. [[CrossRef](#)]
137. Baret, F.; Hagolle, O.; Geiger, B.; Bicheron, P.; Miras, B.; Huc, M.; Berthelot, B.; Niño, F.; Weiss, M.; Samain, O. LAI, fAPAR and fCover CYCLOPES global products derived from VEGETATION: Part 1: Principles of the algorithm. *Remote Sens. Environ.* **2007**, *110*, 275–286. [[CrossRef](#)]
138. Lam, N.S.N.; Quattrochi, D.A. On the issues of scale, resolution, and fractal analysis in the mapping sciences. *Prof. Geogr.* **1992**, *44*, 88–98. [[CrossRef](#)]
139. Rao, N.R.; Garg, P.; Ghosh, S. The effect of radiometric resolution on the retrieval of leaf area index from agricultural crops. *GISci. Remote Sens.* **2006**, *43*, 377–387. [[CrossRef](#)]
140. Haboudane, D.; Miller, J.R.; Pattey, E.; Zarco-Tejada, P.J.; Strachan, I.B. Hyperspectral vegetation indices and novel algorithms for predicting green LAI of crop canopies: Modeling and validation in the context of precision agriculture. *Remote Sens. Environ.* **2004**, *90*, 337–352. [[CrossRef](#)]
141. Lee, K.-S.; Cohen, W.B.; Kennedy, R.E.; Maiersperger, T.K.; Gower, S.T. Hyperspectral versus multispectral data for estimating leaf area index in four different biomes. *Remote Sens. Environ.* **2004**, *91*, 508–520. [[CrossRef](#)]
142. Pu, R.; Yu, Q.; Gong, P.; Biging, G. EO-1 Hyperion, ALI and Landsat 7 ETM+ data comparison for estimating forest crown closure and leaf area index. *Int. J. Remote Sens.* **2005**, *26*, 457–474. [[CrossRef](#)]
143. Vyas, D.; Christian, B.; Krishnayya, N. Canopy level estimations of chlorophyll and LAI for two tropical species (teak and bamboo) from Hyperion (EO1) data. *Int. J. Remote Sens.* **2013**, *34*, 1676–1690. [[CrossRef](#)]
144. Transon, J.; D’Andrimont, R.; Maugnard, A.; Defourny, P. Survey of Hyperspectral Earth Observation Applications from Space in the Sentinel-2 Context. *Remote Sens.* **2018**, *10*, 157. [[CrossRef](#)]
145. Twele, A.; Erasmi, S.; Kappas, M. Spatially explicit estimation of leaf area index using EO-1 Hyperion and Landsat ETM+ data: Implications of spectral bandwidth and shortwave infrared data on prediction accuracy in a tropical montane environment. *GISci. Remote Sens.* **2008**, *45*, 229–248. [[CrossRef](#)]
146. Gong, P.; Pu, R.; Biging, G.S.; Larrieu, M.R. Estimation of forest leaf area index using vegetation indices derived from Hyperion hyperspectral data. *IEEE Trans. Geosci. Remote Sens.* **2003**, *41*, 1355–1362. [[CrossRef](#)]
147. Yuan, H.; Yang, G.; Li, C.; Wang, Y.; Liu, J.; Yu, H.; Feng, H.; Xu, B.; Zhao, X.; Yang, X. Retrieving soybean leaf area index from unmanned aerial vehicle hyperspectral remote sensing: Analysis of RF, ANN, and SVM regression models. *Remote Sens.* **2017**, *9*, 309. [[CrossRef](#)]
148. Thenkabail, P.S. *Remotely Sensed Data Characterization, Classification, and Accuracies*; CRC Press: Boca Raton, FL, USA, 2015. [[CrossRef](#)]
149. Wu, L.; Qin, Q.; Liu, X.; Ren, H.; Wang, J.; Zheng, X.; Ye, X.; Sun, Y. Spatial up-scaling correction for leaf area index based on the fractal theory. *Remote Sens.* **2016**, *8*, 197. [[CrossRef](#)]
150. Garrigues, S.; Allard, D.; Baret, F.; Weiss, M. Quantifying spatial heterogeneity at the landscape scale using variogram models. *Remote Sens. Environ.* **2006**, *103*, 81–96. [[CrossRef](#)]
151. Denny, C.K.; Nielsen, S.E. Spatial Heterogeneity of the Forest Canopy Scales with the Heterogeneity of an Understory Shrub Based on Fractal Analysis. *Forests* **2017**, *8*, 146. [[CrossRef](#)]
152. Frazer, G.W.; Wulder, M.A.; Niemann, K.O. Simulation and quantification of the fine-scale spatial pattern and heterogeneity of forest canopy structure: A lacunarity-based method designed for analysis of continuous canopy heights. *For. Ecol. Manag.* **2005**, *214*, 65–90. [[CrossRef](#)]
153. Zhang, Y.; Yan, G.; Bai, Y. Sensitivity of topographic correction to the DEM spatial scale. *IEEE Geosci. Remote Sens. Lett.* **2014**, *12*, 53–57. [[CrossRef](#)]
154. Friedl, M.; Davis, F.; Michaelsen, J.; Moritz, M. Scaling and uncertainty in the relationship between the NDVI and land surface biophysical variables: An analysis using a scene simulation model and data from FIFE. *Remote Sens. Environ.* **1995**, *54*, 233–246. [[CrossRef](#)]

155. Chen, J.M.; Pavlic, G.; Brown, L.; Cihlar, J.; Leblanc, S.; White, H.; Hall, R.; Peddle, D.; King, D.; Trofymow, J. Derivation and validation of Canada-wide coarse-resolution leaf area index maps using high-resolution satellite imagery and ground measurements. *Remote Sens. Environ.* **2002**, *80*, 165–184. [[CrossRef](#)]
156. Tian, Y.; Woodcock, C.E.; Wang, Y.; Privette, J.L.; Shabanov, N.V.; Zhou, L.; Zhang, Y.; Buermann, W.; Dong, J.; Veikkanen, B. Multiscale analysis and validation of the MODIS LAI product: I. Uncertainty assessment. *Remote Sens. Environ.* **2002**, *83*, 414–430. [[CrossRef](#)]
157. Tian, Y.; Woodcock, C.E.; Wang, Y.; Privette, J.L.; Shabanov, N.V.; Zhou, L.; Zhang, Y.; Buermann, W.; Dong, J.; Veikkanen, B. Multiscale analysis and validation of the MODIS LAI product: II. Sampling strategy. *Remote Sens. Environ.* **2002**, *83*, 431–441. [[CrossRef](#)]
158. Weiss, M.; de Beaufort, L.; Baret, F.; Allard, D.; Bruguier, N.; Marloie, O. Mapping leaf area index measurements at different scales for the validation of large swath satellite sensors: First results of the VALERI project. In Proceedings of the 8th International Symposium in Physical Measurements and Remote Sensing, Aussois, France, 8–12 January 2001; pp. 125–130.
159. Baret, F.; Weiss, M.; Allard, D.; Garrigues, S.; Leroy, M.; Jeanjean, H.; Fernandes, R.; Myneni, R.; Privette, J.; Morissette, J. VALERI: A network of sites and a methodology for the validation of medium spatial resolution land satellite products. *Remote Sens. Environ.* **2005**, *76*, 36–39.
160. Xu, B.; Li, J.; Park, T.; Liu, Q.; Zeng, Y.; Yin, G.; Zhao, J.; Fan, W.; Yang, L.; Knyazikhin, Y. An integrated method for validating long-term leaf area index products using global networks of site-based measurements. *Remote Sens. Environ.* **2018**, *209*, 134–151. [[CrossRef](#)]
161. Zhang, J.; Atkinson, P.; Goodchild, M.F. *Scale in Spatial Information and Analysis*; CRC Press: Boca Raton, FL, USA, 2017. [[CrossRef](#)]
162. Wu, J.; Li, H. Concepts of scale and scaling. In *Scaling and Uncertainty Analysis in Ecology*; Springer: Dordrecht, The Netherlands, 2006; pp. 3–15. [[CrossRef](#)]
163. Fernandes, R.A.; Miller, J.R.; Chen, J.M.; Rubinstein, I.G. Evaluating image-based estimates of leaf area index in boreal conifer stands over a range of scales using high-resolution CASI imagery. *Remote Sens. Environ.* **2004**, *89*, 200–216. [[CrossRef](#)]
164. Ganguly, S.; Samanta, A.; Schull, M.A.; Shabanov, N.V.; Milesi, C.; Nemani, R.R.; Knyazikhin, Y.; Myneni, R.B. Generating vegetation leaf area index Earth system data record from multiple sensors. Part 2: Implementation, analysis and validation. *Remote Sens. Environ.* **2008**, *112*, 4318–4332. [[CrossRef](#)]
165. Goodchild, M.F. Scale in GIS: An overview. *Geomorphology* **2011**, *130*, 5–9. [[CrossRef](#)]
166. Soudani, K.; François, C.; Le Maire, G.; Le Dantec, V.; Dufrêne, E. Comparative analysis of IKONOS, SPOT, and ETM+ data for leaf area index estimation in temperate coniferous and deciduous forest stands. *Remote Sens. Environ.* **2006**, *102*, 161–175. [[CrossRef](#)]
167. Schulze, E. Plant life forms and their carbon, water and nutrient relations. In *Physiological Plant Ecology II*; Springer: Berlin/Heidelberg, Germany, 1982; pp. 615–676. [[CrossRef](#)]
168. Thomas, S.C.; Winner, W.E. Leaf area index of an old-growth Douglas-fir forest estimated from direct structural measurements in the canopy. *Can. J. For. Res.* **2000**, *30*, 1922–1930. [[CrossRef](#)]
169. Beadle, C.L. Growth analysis. In *Photosynthesis and Production in a Changing Environment: A Field and Laboratory Manual*; Hall, D.O., Scurlock, J.M.O., Bolhàr-Nordenkampf, H.R., Leegood, R.C., Long, S.P., Eds.; Springer: Dordrecht, The Netherlands, 1993; pp. 36–46. [[CrossRef](#)]
170. Colombo, R.; Bellingeri, D.; Fasolini, D.; Marino, C.M. Retrieval of leaf area index in different vegetation types using high resolution satellite data. *Remote Sens. Environ.* **2003**, *86*, 120–131. [[CrossRef](#)]
171. Zhou, J.; Zhao, Z.; Zhao, J.; Zhao, Q.; Wang, F.; Wang, H. A comparison of three methods for estimating the LAI of black locust (*Robinia pseudoacacia* L.) plantations on the Loess Plateau, China. *Int. J. Remote Sens.* **2014**, *35*, 171–188. [[CrossRef](#)]
172. Wu, J.; Wang, D.; Bauer, M.E. Assessing broadband vegetation indices and QuickBird data in estimating leaf area index of corn and potato canopies. *Field Crops Res.* **2007**, *102*, 33–42. [[CrossRef](#)]
173. Tillack, A.; Clasen, A.; Kleinschmit, B.; Förster, M. Estimation of the seasonal leaf area index in an alluvial forest using high-resolution satellite-based vegetation indices. *Remote Sens. Environ.* **2014**, *141*, 52–63. [[CrossRef](#)]
174. Dong, T.; Liu, J.; Shang, J.; Qian, B.; Ma, B.; Kovacs, J.M.; Walters, D.; Jiao, X.; Geng, X.; Shi, Y. Assessment of red-edge vegetation indices for crop leaf area index estimation. *Remote Sens. Environ.* **2019**, *222*, 133–143. [[CrossRef](#)]

175. Liang, S.; Fang, H.; Kaul, M.; Van Niel, T.G.; McVicar, T.R.; Pearlman, J.S.; Walthall, C.L.; Daughtry, C.S.; Huemmrich, K.F. Estimation and validation of land surface broadband albedos and leaf area index from EO-1 ALI data. *IEEE Trans. Geosci. Remote Sens.* **2003**, *41*, 1260–1267. [[CrossRef](#)]
176. Menzies, J.; Jensen, R.; Brondizio, E.; Moran, E.; Mausel, P. Accuracy of neural network and regression leaf area estimators for the Amazon Basin. *GISci. Remote Sens.* **2007**, *44*, 82–92. [[CrossRef](#)]
177. Han, W.; Qu, Y. Data Uncertainty in an Improved Bayesian Network and Evaluations of the Credibility of the Retrieved Multitemporal High-Spatial-Resolution Leaf Area Index (LAI). *IEEE J. Sel. Top. Appl. Earth Obs. Remote Sens.* **2016**, *9*, 3553–3563. [[CrossRef](#)]
178. Wang, X.Y.; Qin, W.H.; Sun, G.Q.; Zhu, J. Estimation of forest LAI by inverting canopy reflectance models and multi-angle imagery. *Geocarto Int.* **2018**, *34*, 959–976. [[CrossRef](#)]
179. Vuolo, F.; Neugebauer, N.; Bolognesi, S.; Atzberger, C.; D’Urso, G. Estimation of leaf area index using DEIMOS-1 data: Application and transferability of a semi-empirical relationship between two agricultural areas. *Remote Sens.* **2013**, *5*, 1274–1291. [[CrossRef](#)]
180. Wu, C.; Han, X.; Niu, Z.; Dong, J. An evaluation of EO-1 hyperspectral Hyperion data for chlorophyll content and leaf area index estimation. *Int. J. Remote Sens.* **2010**, *31*, 1079–1086. [[CrossRef](#)]
181. He, L.; Chen, Z.; Jiang, Z.; Wu, W.; Ren, J.; Bin, L.; Tuya, H. Comparative analysis of GF-1, HJ-1, and Landsat-8 data for estimating the leaf area index of winter wheat. *J. Integr. Agric.* **2017**, *16*, 266–285. [[CrossRef](#)]
182. Rao, N.R.; Garg, P.; Ghosh, S. Estimation and comparison of leaf area index of agricultural crops using IRS LISS-III and EO-1 Hyperion images. *J. Indian Soc. Remote Sens.* **2006**, *34*, 69–78. [[CrossRef](#)]
183. Blinn, C.E.; House, M.N.; Wynne, R.H.; Thomas, V.A.; Fox, T.R.; Sumnall, M. Landsat 8 based leaf area index estimation in loblolly pine plantations. *Forests* **2019**, *10*, 222. [[CrossRef](#)]
184. Pasqualotto, N.; Delegido, J.; Van Wittenberghe, S.; Rinaldi, M.; Moreno, J. Multi-Crop green LAI estimation with a new simple Sentinel-2 LAI index (SeLI). *Sensors* **2019**, *19*, 904. [[CrossRef](#)]
185. Gu, Z.; Shi, X.; Li, L.; Yu, D.; Liu, L.; Zhang, W. Using multiple radiometric correction images to estimate leaf area index. *Int. J. Remote Sens.* **2011**, *32*, 9441–9454. [[CrossRef](#)]
186. Houborg, R.; Anderson, M.; Daughtry, C. Utility of an image-based canopy reflectance modeling tool for remote estimation of LAI and leaf chlorophyll content at the field scale. *Remote Sens. Environ.* **2009**, *113*, 259–274. [[CrossRef](#)]
187. Wang, Q.; Adiku, S.; Tenhunen, J.; Granier, A. On the relationship of NDVI with leaf area index in a deciduous forest site. *Remote Sens. Environ.* **2005**, *94*, 244–255. [[CrossRef](#)]
188. Alexandridis, T.K.; Ovakoglou, G.; Clevers, J.G. Relationship between MODIS EVI and LAI across time and space. *Geocarto Int.* **2019**, *1*–15. [[CrossRef](#)]
189. Jin, X.; Yang, G.; Xu, X.; Yang, H.; Feng, H.; Li, Z.; Shen, J.; Lan, Y.; Zhao, C. Combined multi-temporal optical and radar parameters for estimating LAI and biomass in winter wheat using HJ and RADARSAR-2 data. *Remote Sens.* **2015**, *7*, 13251–13272. [[CrossRef](#)]
190. Zhao, K.; Popescu, S. Lidar-based mapping of leaf area index and its use for validating GLOBCARBON satellite LAI product in a temperate forest of the southern USA. *Remote Sens. Environ.* **2009**, *113*, 1628–1645. [[CrossRef](#)]
191. Luo, S.; Wang, C.; Li, G.; Xi, X. Forest leaf area index (LAI) estimation using airborne discrete-return lidar data. *Chin. J. Geophys.* **2013**, *56*, 233–242. [[CrossRef](#)]
192. Wu, C.; Niu, Z.; Tang, Q.; Huang, W. Estimating chlorophyll content from hyperspectral vegetation indices: Modeling and validation. *Agric. For. Meteorol.* **2008**, *148*, 1230–1241. [[CrossRef](#)]
193. Brown, L.; Chen, J.M.; Leblanc, S.G.; Cihlar, J. A shortwave infrared modification to the simple ratio for LAI retrieval in boreal forests: An image and model analysis. *Remote Sens. Environ.* **2000**, *71*, 16–25. [[CrossRef](#)]
194. Chen, J.M. Evaluation of vegetation indices and a modified simple ratio for boreal applications. *Can. J. Remote Sens.* **1996**, *22*, 229–242. [[CrossRef](#)]
195. He, L.; Coburn, C.A.; Wang, Z.-J.; Feng, W.; Guo, T.-C. Reduced prediction saturation and view effects for estimating the leaf area index of winter wheat. *IEEE Trans. Geosci. Remote Sens.* **2019**, *57*, 1637–1652. [[CrossRef](#)]
196. Heiskanen, J.; Rautiainen, M.; Korhonen, L.; Möttus, M.; Stenberg, P. Retrieval of boreal forest LAI using a forest reflectance model and empirical regressions. *Int. J. Appl. Earth Obs. Geoinf.* **2011**, *13*, 595–606. [[CrossRef](#)]

197. Sonobe, R.; Wang, Q. Hyperspectral indices for quantifying leaf chlorophyll concentrations performed differently with different leaf types in deciduous forests. *Ecol. Inform.* **2017**, *37*, 1–9. [[CrossRef](#)]
198. Combal, B.; Baret, F.; Weiss, M.; Trubuil, A.; Mace, D.; Pragnere, A.; Myneni, R.; Knyazikhin, Y.; Wang, L. Retrieval of canopy biophysical variables from bidirectional reflectance: Using prior information to solve the ill-posed inverse problem. *Remote Sens. Environ.* **2003**, *84*, 1–15. [[CrossRef](#)]
199. Li, P.; Wang, Q. Retrieval of leaf biochemical parameters using PROSPECT inversion: A new approach for alleviating ill-posed problems. *IEEE Trans. Geosci. Remote Sens.* **2011**, *49*, 2499–2506. [[CrossRef](#)]
200. Meroni, M.; Colombo, R.; Panigada, C. Inversion of a radiative transfer model with hyperspectral observations for LAI mapping in poplar plantations. *Remote Sens. Environ.* **2004**, *92*, 195–206. [[CrossRef](#)]
201. Rivera, J.P.; Verrelst, J.; Leonenko, G.; Moreno, J. Multiple cost functions and regularization options for improved retrieval of leaf chlorophyll content and LAI through inversion of the PROSAIL model. *Remote Sens.* **2013**, *5*, 3280–3304. [[CrossRef](#)]
202. Verrelst, J.; Malenovský, Z.; Van der Tol, C.; Camps-Valls, G.; Gastellu-Etchegorry, J.P.; Lewis, P.; North, P.; Moreno, J. Quantifying Vegetation Biophysical Variables from Imaging Spectroscopy Data: A Review on Retrieval Methods. *Surv. Geophys.* **2019**, *40*, 589–629. [[CrossRef](#)]
203. Jin, H.; Xu, W.; Li, A.; Xie, X.; Zhang, Z.; Xia, H. Spatially and temporally continuous leaf area index mapping for crops through assimilation of multi-resolution satellite data. *Remote Sens.* **2019**, *11*, 2517. [[CrossRef](#)]
204. Fang, H.; Wei, S.; Jiang, C.; Scipal, K. Theoretical uncertainty analysis of global MODIS, CYCLOPES, and GLOBCARBON LAI products using a triple collocation method. *Remote Sens. Environ.* **2012**, *124*, 610–621. [[CrossRef](#)]
205. Richardson, A.D.; Dail, D.B.; Hollinger, D. Leaf area index uncertainty estimates for model–data fusion applications. *Agric. For. Meteorol.* **2011**, *151*, 1287–1292. [[CrossRef](#)]
206. Wang, Y.; Tian, Y.; Zhang, Y.; El-Saleous, N.; Knyazikhin, Y.; Vermote, E.; Myneni, R.B. Investigation of product accuracy as a function of input and model uncertainties: Case study with SeaWiFS and MODIS LAI/FPAR algorithm. *Remote Sens. Environ.* **2001**, *78*, 299–313. [[CrossRef](#)]
207. Fang, H.; Jiang, C.; Li, W.; Wei, S.; Baret, F.; Chen, J.M.; Garcia-Haro, J.; Liang, S.; Liu, R.; Myneni, R.B. Characterization and intercomparison of global moderate resolution leaf area index (LAI) products: Analysis of climatologies and theoretical uncertainties. *J. Geophys. Res. Biogeosci.* **2013**, *118*, 529–548. [[CrossRef](#)]
208. Wulder, M.A.; Loveland, T.R.; Roy, D.P.; Crawford, C.J.; Masek, J.G.; Woodcock, C.E.; Allen, R.G.; Anderson, M.C.; Belward, A.S.; Cohen, W.B.; et al. Current status of Landsat program, science, and applications. *Remote Sens. Environ.* **2019**, *225*, 127–147. [[CrossRef](#)]
209. Main-Knorn, M.; Pflug, B.; Louis, J.; Debaecker, V.; Müller-Wilm, U.; Gascon, F. Sen2Cor for Sentinel-2. In Proceedings of the SPIE Image and Signal Processing for Remote Sensing XXIII, Warsaw, Poland, 11–13 September 2017. [[CrossRef](#)]
210. Foody, G.M.; Atkinson, P.M. *Uncertainty in Remote Sensing and GIS*; John Wiley & Sons: Hoboken, NJ, USA, 2003. [[CrossRef](#)]
211. Yao, Y.; Liu, Q.; Liu, Q.; Li, X. The LAI Inversion Uncertainties in Heterogeneous Surface. In Proceedings of the 2006 IEEE International Symposium on Geoscience and Remote Sensing, Denver, CO, USA, 31 July–4 August 2006; pp. 2689–2692.
212. Matsushita, B.; Yang, W.; Chen, J.; Onda, Y.; Qiu, G. Sensitivity of the Enhanced Vegetation Index (EVI) and Normalized Difference Vegetation Index (NDVI) to topographic effects: A case study in high-density Cypress forest. *Sensors* **2007**, *7*, 2636–2651. [[CrossRef](#)]
213. Jin, H.; Li, A.; Xu, W.; Xiao, Z.; Jiang, J.; Xue, H. Evaluation of topographic effects on multiscale leaf area index estimation using remotely sensed observations from multiple sensors. *ISPRS J. Photogramm. Remote Sens.* **2019**, *154*, 176–188. [[CrossRef](#)]
214. Yao, Y.; Liu, Q.; Liu, Q.; Li, X. LAI retrieval and uncertainty evaluations for typical row-planted crops at different growth stages. *Remote Sens. Environ.* **2008**, *112*, 94–106. [[CrossRef](#)]
215. Pisek, J.; Chen, J.M. Mapping forest background reflectivity over North America with Multi-angle Imaging SpectroRadiometer (MISR) data. *Remote Sens. Environ.* **2009**, *113*, 2412–2423. [[CrossRef](#)]
216. Verrelst, J.; Rivera, J.P.; Moreno, J.; Camps-Valls, G. Gaussian processes uncertainty estimates in experimental Sentinel-2 LAI and leaf chlorophyll content retrieval. *ISPRS J. Photogramm. Remote Sens.* **2013**, *86*, 157–167. [[CrossRef](#)]

217. Qu, Y.; Han, W.; Ma, M. Retrieval of a temporal high-resolution leaf area index (LAI) by combining MODIS LAI and ASTER reflectance data. *Remote Sens.* **2015**, *7*, 195–210. [[CrossRef](#)]
218. Varvia, P.; Rautiainen, M.; Seppänen, A. Modeling uncertainties in estimation of canopy LAI from hyperspectral remote sensing data—A Bayesian approach. *J. Quant. Spectrosc. Radiat. Transf.* **2017**, *191*, 19–29. [[CrossRef](#)]



© 2020 by the authors. Licensee MDPI, Basel, Switzerland. This article is an open access article distributed under the terms and conditions of the Creative Commons Attribution (CC BY) license (<http://creativecommons.org/licenses/by/4.0/>).